# 10. ORGANIC GEOCHEMISTRY AND SEDIMENTOLOGY OF LOWER TO MID-CRETACEOUS DEEP-SEA CARBONATES, SITES 535 AND 540, LEG 77[1]

J. W. Patton, P. W. Choquette, G. K. Guennel, A. J. Kaltenback, and A. Moore, Marathon Oil Company, Denver Research Center, Littleton, Colorado


## ABSTRACT

Analyses of 40 carbonate core samples—27 from Site 535, 12 from Site 540, and 1 from Site 538A—have confirmed many of the findings of the Shipboard Scientific Party. The samples, all but one Early to mid-Cretaceous in age (Berriasian to Cenomanian), reflect sequences of cyclically anoxic and oxic depositional environments. They are moderately to very dark colored, dominantly planar-parallel, laminated lime mudstones. Most show the effects of intense mechanical compaction.

Visual kerogen characteristics and conventional Rock-Eval parameters indicate that these deep basinal carbonates contain varying mixtures of thermally immature kerogen derived from both marine and terrigenous precursors. However, variations in kerogen chemistry are evident upon analysis of the pyrolysis mass spectral data in conjunction with the other geochemical analyses. Particularly diagnostic is the reduction index, RI, a measure of $H_2S$ produced during pyrolysis. Total organic carbon, TOC, ranges from 0.6 to 6.6%, with an overall average of 2.4%. Average TOCs for these fine-grained mudstones are: late Eocene 2.5% (1 sample), Cenomanian 2.2% (6), Albian 2.0% (10), Aptian 1.3% (1), Barremian-Hauterivian 2.8% (11), late Valanginian 4.8% (3), Berriasian–early Valanginian 1.6% (7).

Most of the carbonates have source-potential ratings of fair to very good of predominantly oil-prone to mixed kerogen, with only a few gas-prone samples. The ratings correlate well with the inferred depositional environments, i.e., whether oxic or anoxic. Several new organic-geochemical parameters, especially RI, based on pyrolysis mass spectrometry of powdered whole-rock samples, support this view.

Tar from fractures in laminated to bioturbated limestones of Unit IV (late Valanginian) at 535-58-4, 19–20 cm (530 m sub-bottom) appears to be mature, biodegraded, and of migrated rather than on site indigenous origin.


## INTRODUCTION

The 40 carbonate core samples used in this study represent a sampling of the dark-colored, deep-marine lime mudstones from three holes on Leg 77 (Fig. 1): 535 (Samples 1–26), 538A (27), and 540 (28–39). Sample 40 is tar from Site 535. As summarized in Table 1, the one sample from Hole 538A is from a sequence dated as late Eocene; all the others represent units of Early to mid-Cretaceous age.

In order to assure ample organic matter, relatively dark-colored carbonates were selected in shipboard work done in collaboration with L. B. Magoon III. This introduced a bias toward a sampling of sediments deposited under relatively anoxic conditions, and indeed our data show good correlation between anoxic conditions and organic matter preservation. This is consistent with views expressed by Arthur and Schlager (1979), Demaison and Moore (1980), Tissot et al. (1980), and Schlager and others (1983).

Despite some stratigraphic omissions, this suite of samples gives a reasonably good representation of the darker Lower Cretaceous to mid-Cretaceous mudrocks in the composite section provided by Sites 535 and 540.

Pyrolysis mass spectrometry (Patton and Moore, 1982), conventional organic geochemical analyses, visual kerogen assessment, thin-section petrography, and X-ray diffraction analyses of bulk crushed samples were the principal approaches used in this study. Several new geochemical parameters based on pyrolysis mass-spectral data are introduced.

### EXPERIMENTAL APPROACHES

Carbon analyses were determined by Huffman Laboratories, Wheatridge, Colorado, and Rock-Eval data for these samples were supplied by Dr. G. E. Claypool, U.S. Geological Survey, Denver, Colorado. All other analyses were performed at Marathon Oil Company's Denver Research Center.

Isotopic carbon data were determined with a Nuclide RMS 6–60° isotope-ratio mass spectrometer. All isotopic carbon data are referred to PDB as a standard. Appendixes A–C summarize the basic organic geochemical data, and Appendixes D and E as noted later, summarize the basic kerogen and inorganic compositional data.

Thermolyses of whole-rock samples were performed with a Varian CH-5 mass spectrometer. Samples were heated in a special probe at 20°C/minute from an initial temperature of 30°C to a maximum temperature of 750°C, and mass scans were taken at every 5°C increase in temperature. This technique is similar to that reported by Souron and others (1974). The data obtained were ultimately stored on magnetic tape for processing with a Burroughs 6800 computer.

A convenient way to visualize the resulting data is by making orthographic plots of Z values versus thermolysis temperature. Z represents a parameter in the general empirical formula for hydrocarbons, $C_nH_{2n+Z}$, where Z ranges from $-11$ to $+2$. All hydrocarbons can be fitted to the above empirical formula. The subscript on the carbon, n, is the number of carbon atoms in the particular molecule in question. The subscript on the hydrogen, $2n+Z$, is the number of hydrogen atoms. The value of Z serves to distinguish different classes of hydrocarbons from one another. For example, all paraffins fit the empirical formula $C_nH_{2n+2}$. This is a special case where $Z = +2$. Monocyclic paraffins are in the class where $Z = 0$, dicyclic paraffins fit $Z = -2$, benzenes fit $Z = -6$, and benzodicycloparaffins fit $Z = -10$ just to mention a few. In such a data reduction, certain masses for inorganic gases (18 for water, 34 for hydrogen sulfide, 44 for carbon dioxide, etc.) must be removed. Species containing heteroatoms (e.g., O, N,

[1] Buffler, R. T., Schlager, W., et al., *Init. Repts. DSDP*, 77: Washington (U.S. Govt. Printing Office).

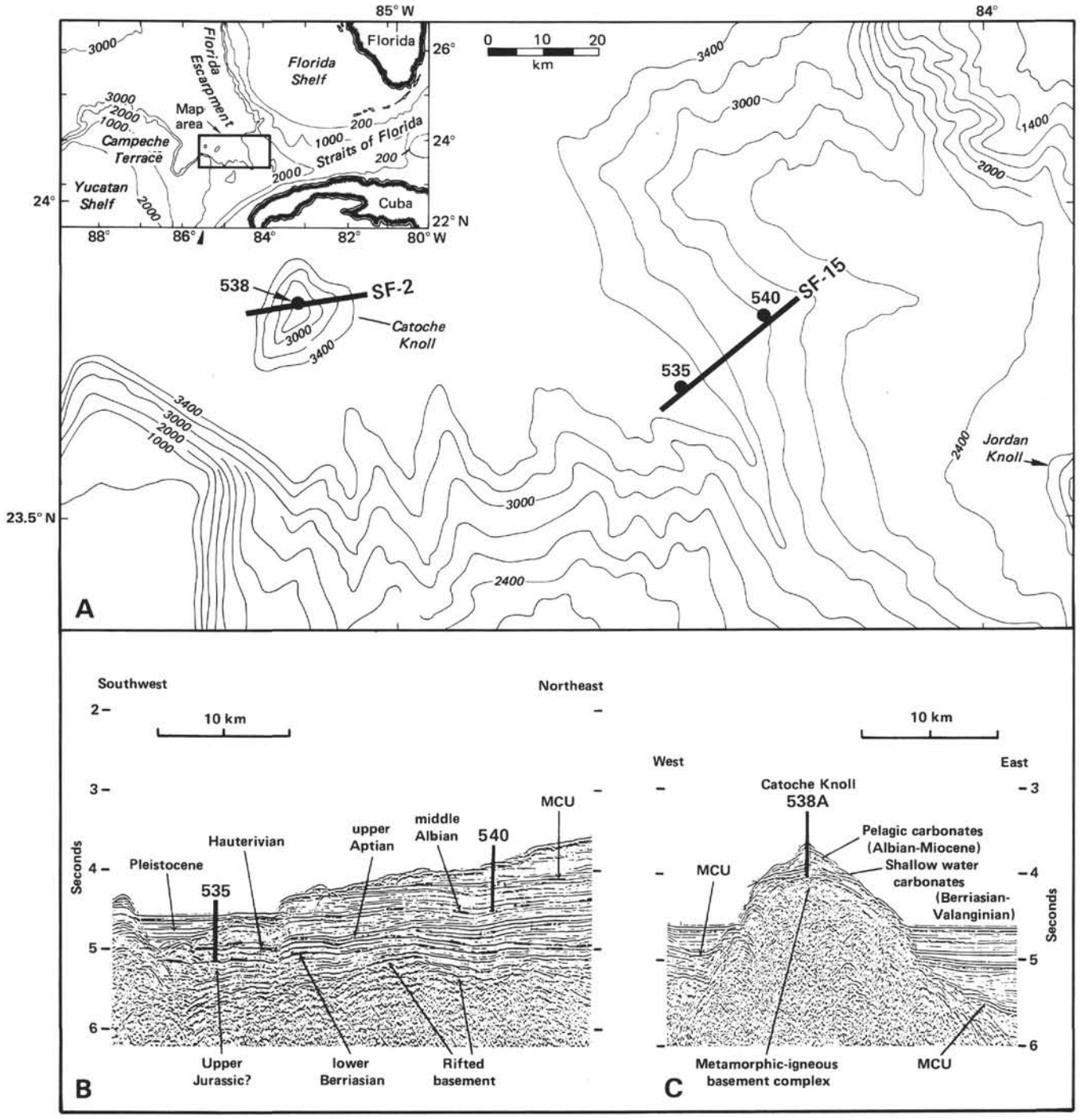


Figure 1. A. Location and seismic stratigraphy of sites studied. B and C. Seismic record sections SF-15 and SF-2 respectively. (After Schlager et al., in press.) MCU = mid-Cretaceous unconformity.

and S) are treated as if they were true hydrocarbons. Consequently, the resulting data reduction only gives an approximation as to the chemical make-up of the species detected in the mass spectrometer.

Figure 2 shows some examples of the resulting orthographic plots of the Z data. This is particularly useful because it readily shows different temperature regions of interest. The range from 30 to 300°C represents a region where volatile hydrocarbons appear, comparable to material that could be solvent extracted. The range from 300 to 600°C represents the pyrolysis (cracking) region that produces oil-like material, and above that to 750°C, the dry-gas cracking region.

Sample 1 illustrates the absence of extractable material (no material in the 30 to 300°C range), showing only hydrocarbons derived by cracking the kerogen (Fig. 2A). Sample 16, in contrast, shows significant amounts of hydrocarbons in this low-temperature zone (Fig. 2B). Sample 19 shows a bimodal distribution in the cracking region, suggesting a mixture of two or more types of organic matter (Fig. 2C). This is consistent with the visual kerogen assessment (see discussion in a later section).

Sample 27 (Fig. 2D) shows the appearance of material above 600°C that represents the dry-gas cracking region commonly seen in the pyrolysis of coals.

Although useful for visualizing the mountain of data obtained from the thermolysis of the samples, a quantitative analysis is difficult without further data reduction. Yet this approach does show distinct

Table 1. Petrographic descriptions of samples for organic-geochemical analysis, grouped by age and lithostratigraphic unit.

| Sample number | Hole-Core-Section (interval in cm) | Age | Shipboard lithologic unit | Description |
|---|---|---|---|---|
| 27 | 538A-16-5, 21–27 | late Eocene | Unit II | Siliceous lime WS, poorly laminated, with abundant, slightly to completely dissolved radiolarians and diatoms; matrix strongly compacted but siliceous organisms uncrushed; no molds are silica filled. |
| 28<br>29 | 540-37-1, 44–53<br>540-37-2, 46–55 | early Cenomanian | Uppermost Unit IV | Laminated lime MS, 5Y 7/1 (Sample 28) to 5Y 5/1-6/1 (Sample 29); abundant planktonic foraminifers and organic matter in Sample 29; chalcedonic-quartz–filled molds of radiolarians(?) abundant in a few mm laminae interspersed with rather featureless lime mudstone (micrite); foraminifers empty or barely lined with calcite microspar, and unbroken despite severe compaction of surrounding micrite (especially in Sample 29). |
| 30<br>31<br>32<br>33<br>34 | 540-42-2, 27–34<br>540-43-2, 60–60<br>540-44-2, 74–77<br>540-45-1, 50–58<br>540-45-2, 93–100 | latest Albian | Middle of Unit IV | Laminated lime MS as above, but without radiolarians; planktonic foraminifers rare to very abundant (15–20%), empty or filled with "dirty-appearing" chalcedonic quartz; planktonic foraminifers uncrushed; "smeared-out," highly elongate compacted micrite pellets, with length-to-width ratios up to 10:1. |
| 35<br>36<br>37<br>38<br>39 | 540-46-1, 74–80<br>540-47-1, 78–84<br>540-48-1, 138–142<br>540-50-2, 38–52<br>540-63-1, 80–86 | late Albian | Middle and lower parts of Unit IV (except Sample 39, Subunit Va) | Laminated to streaky laminated WS/PS and (Sample 38) MS, 5Y 4/1 (moderately dark) to 5Y 6/1-7/1 (light), with sparser planktonic foraminifers than above (Samples 29–34), but relatively abundant uncompacted pellets of micrite; abundances of pellets correlate crudely with organic carbon contents, $S_1$ and $S_2$; moderately to strongly compacted. |
| 1<br>2 | 535-31-7, 0–14<br>535-35-5, 6–20 | Cenomanian(?) | Upper part of Unit II | Lime MS with sparce calcispheres (Sample 1) and laminated WS/PS with rare phosphate grains and abundant compacted pellets and organic matter (Sample 2); "trains" and isolated crystals of iron sulfides. |
| 3<br>4 | 535-42-5, 120–130<br>535-42-5, 23–32 | Cenomanian(?) | Near base of Unit II | Lime MS, laminated, dark (5Y 4/1-5/1) with rare phosphate grains and unidentified silt-sized bioclastic debris, as well as common compacted pellets; trace–1% dolomite in 10–15 μm rhombs. |
| 5 | 535-44-1, 80–128 | Aptian | Upper part of Unit III | Lime MS-WS, like Sample 4 but with abundant compacted pellets; no planktonic foraminifers, traces of silt-sized phosphate grains. |
| 6<br>7<br>8<br>9 | 535-50-2, 77–96<br>535-50-3, 27–34a<br>535-50-3, 27–34b<br>535-50-3, 27–34c | late Hauterivian | Bottom of Unit III | Lime MS-WS (Samples 6 and 7) as above. Sample 8 is light-colored chert; silicified MS with rare silicified calcispheres and rather abundant grainy organic matter. Sample 9 is very dark (5Y 3/1), organic matter–rich, sulfide-rich MS/WS(?). |
| 10<br>11<br>12<br>13<br>14<br>15<br>16<br>40 | 535-52-1, 69–85<br>535-53-3, 0–32<br>535-43-6, 53–72<br>535-55-4, 51–72<br>535-56-7, 73–87<br>535-58-2, 103–108<br>535-58-4, 3–46<br>535-58-4, 19–20 | early Hauterivian | Upper half of Unit IV | Lime MS-WS for the most part, very evenly laminated, dark to moderately light (5Y 2/1–5Y 6/1), with common to abundant flattened pellets and rare to common (trace–15%) dolomite in the form of dolomitized burrow(?) fillings and scattered rhombs; dolomite is microcrystalline to finely crystalline. Sample 16 is calcisphere MS-WS in which calcite spar fills the calcispheres and only slight compaction is apparent; strongly flattened pellets are abundant in the rest; Sample 40 is tar/asphalt. |
| 17<br>18<br>19 | 535-61-1, 29–42<br>535-63-4, 97–115<br>535-64-4, 60–86 | late Valanginian | Bottom half of Unit IV | Lime MS as above, with common-to-abundant flattened burrows or flattened soft pellets; Sample 21 is like Samples 17–19, and Sample 20 has several percent flattened clay-quartz pellets(?), calcispheres, and unidentified bioclastic grains. |
| 20<br>21 | 535-66-2, 20–39<br>535-67-2, 126–134 | early Valanginian | Base of Unit IV | Lime MS-WS, well laminated; Sample 20 has abundant flattened burrows or pellets (in Sample 21 they are rare); Sample 21 is like Samples 17–19, and Sample 20 has several percent flattened clay-quartz pellets(?), calcispheres, and unidentified bioclastic grains. |
| 22<br>23<br>24<br>25 | 535-68-5, 109–125<br>535-69-5, 60–68<br>535-70-3, 133–148<br>535-71-3, 97–123 | early Valanginian | Upper part of Unit V | Lime MS, rather poorly laminated and in some centimeters burrowed beds; trace to 2–4% siliciclastic, silt-sized grains (quartz and a little clay); pellets rare or absent, no planktonic foraminifers, and trace to 15–20% dolomite; dominantly light colored (5Y 7/1–6/1) with interlaminated dark MS (5Y 4/1–3/1). |
| 26 | 535-78-1, 89–97 | late Berriasian | Unit V | Lime MS similar to Sample 25; 10–15% dolomite; strongly compacted fabric with rare flattened pellets. |

Note: The abbreviations MS, WS, and PS refer to the textural carbonate classification (mudstone, wackestone, and packstone) of Dunham (1962). Ages are based on site chapters, Site 538 and Sites 535, 539, and 540 (this volume). The a, b, and c after cm intervals are piece numbers.

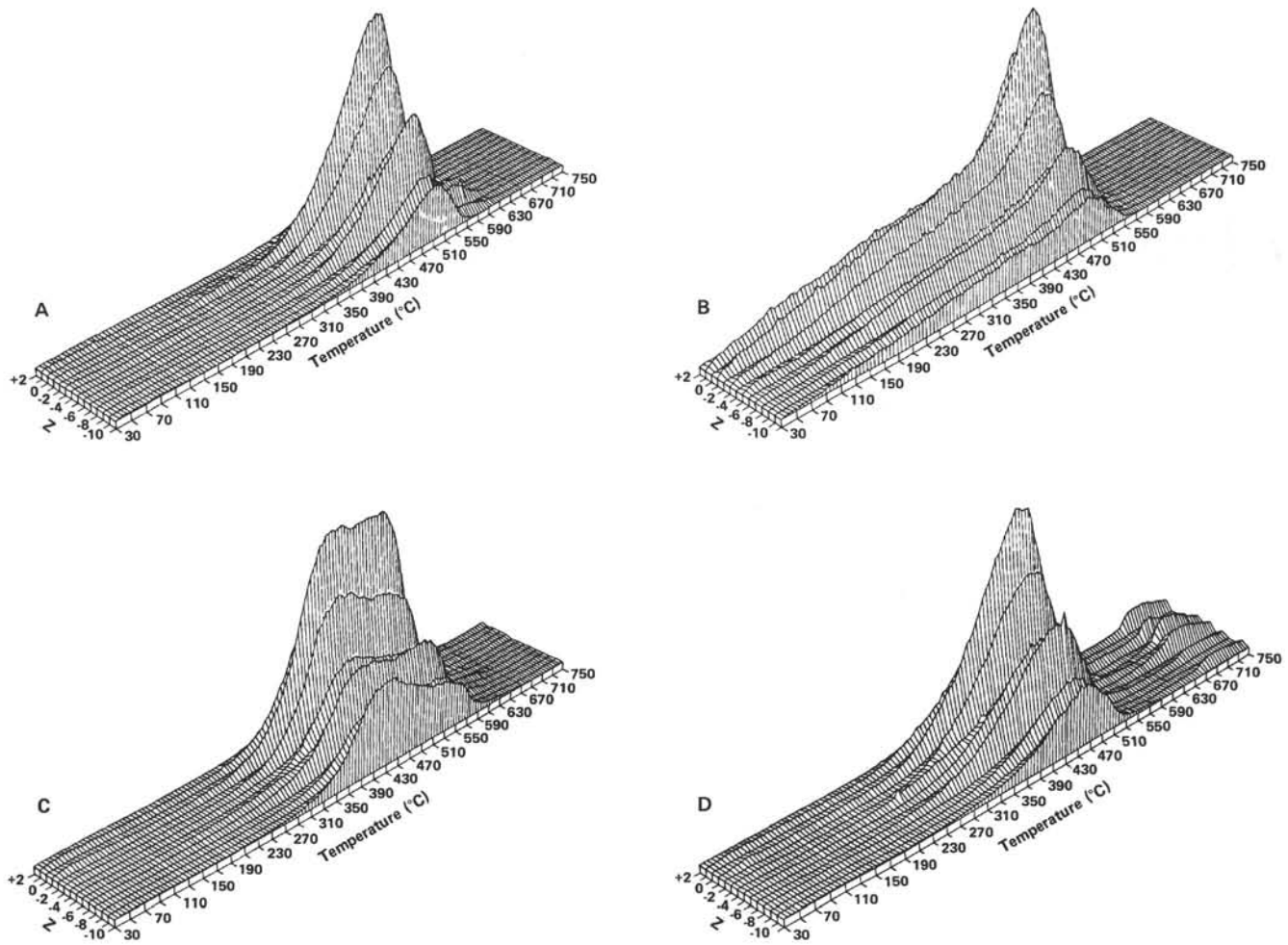


Figure 2. Orthographic plots of pyrolysis/mass spectral Z data versus temperature. Heating rate = 20°C/minute. Masses excluded in calculations are: 17, 18, 19, 22, 28, 29, 30, 32, 33, 34, 44, 45, 46, 48, 64, 65, and 66. (See text for further explanation.) A. Sample 1 (535-31-7, 0–14 cm). B. Sample 16 (535-58-4, 3–46 cm). C. Sample 19 (535-64-4, 60–86 cm). D. Sample 27 (538A-16-5, 21–27 cm).

hydrocarbon groupings characteristic of what we believe to illustrate different types of organic matter in addition to their depositional environments.

One useful approach is to obtain a single mass spectrum corresponding to an average of the pyrolysis temperature zone, from 300 to 600°C, and then subject this average spectrum to a paraffin-naphthene-aromatic (PNA) analysis by the technique of Robinson (1971). Appendix C summarizes such a data reduction.

It must be emphasized that these resulting data do not paint a true picture of the pyrolysis products. Olefins and diolefins are undoubtedly produced in the pyrolysis (cracking) of the kerogen. However, Robinson's Fortran computer program cannot distinguish between an olefin and a monocyclic naphthene, a diolefin and a dicyclic naphthene, and so forth. Nevertheless, these data are useful in distinguishing one pyrolysis sample from another.

The sensitivity of the CH-5 mass spectrometer varied from day to day, primarily because of contamination of the ion source by sulfur compounds. Eventually, when contamination was severe, the source had to be disassembled and cleaned. Therefore, for quantification, a daily response factor was determined by pyrolyzing a standard sample (from the Skull Creek formation, Powder River Basin, Wyoming) at the beginning and end of each day. This enabled us to quantify the mass spectral data.

Several new parameters have been introduced in Appendix C, as a result of this quantitative capability. They are the pyrolysis $S_1$ index ($PS_1$), the pyrolysis $S_2$ index ($PS_2$), the pyrolysis production index (PPI), the pyrolysis hydrocarbon index (PHI), and the reduction index (RI).

$PS_1$ and $PS_2$ are essentially analogous to the Rock-Eval $S_1$ and $S_2$ parameters. The $PS_1$ value was determined from an average mass spectrum from 30 to 300°C, and $PS_2$ from an average spectrum from 300 to 600°C. For each of these pyrolysis parameters, counts of masses representative for paraffins, monocyclic naphthenes, and aromatics per $\mu$g of sample were adjusted by the daily instrument response factor. The masses used for the paraffins were 43 + 57 + 71; those for the monocyclic naphthenes were 41 + 55 + 69; and those for the aromatics were 91 + 141 + 191. PPI is simply $PS_1/(PS_1 + PS_2)$, expressed as a percentage.

PHI is simply $PS_2$ divided by the percent organic carbon in the sample. The resulting PHI values were generally proportional to the hydrogen index values, HI, determined by the Rock-Eval apparatus, and $PS_1$ and $PS_2$ parameters proportional to the $S_1$ and $S_2$ parameters.

RI was obtained by dividing the counts from masses expected for $H_2S$, 33 + 34 + 36, by the sample weight in $\mu$g, and in turn corrected by the response factor using the average spectrum for 300°C to 600°C. Because pyrite in general is minimal in these samples, RI is believed to be a good indicator of the quantity of organic sulfur in the kerogen and to give a general indication of how reducing the depositional environment was. Low values appear to correlate with oxic conditions and higher values with anoxic conditions at the time of deposition.

Sulfur isotopic studies (Orr, 1974) have shown that a large portion of sulfur in petroleum has been derived from reduced sulfur attributed to microbial reduction of sulfate. Thus, larger RI values imply stronger sulfate-reducing conditions at the time of deposition and early diagenesis and hence anoxic marine conditions. A plot of RI versus 1000/oxygen index (Fig. 3) demonstrates the inverse relationship be-

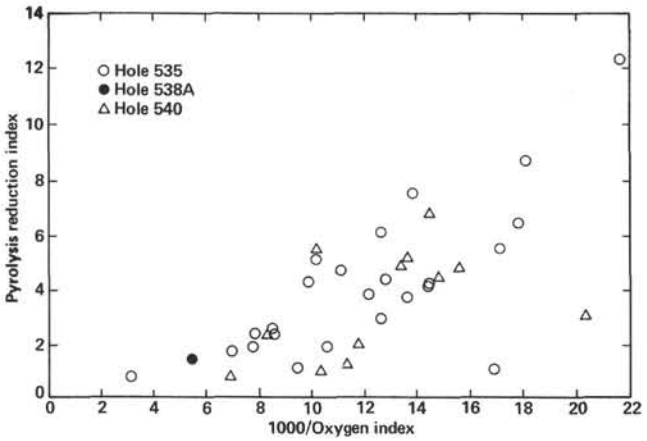


Figure 3. Reduction index (RI) versus the reciprocal of the oxygen index (OI), demonstrating their inverse relationship.

tween the two. That is, small RI values are normally found with high OI values and vice versa.

Our data suggest that RI values ranging from 0.8 to 2.6 (low values) represent oxic conditions; values ranging from 1.0 to 6.1 (intermediate values) indicate a fluctuating or borderline condition between oxic and anoxic conditions; and 4.1 and 15.5 (high) values represent anoxic conditions. We have deliberately overlapped these zones to indicate they are only approximations. Nevertheless these designations are generally consistent with other geochemical parameters such as Rock-Eval oxygen indexes, total organic carbon, and mass spectral PNA values.

No Rock-Eval data are available for Sample 40, the tar/asphalt specimen recovered from Sample 535-58-4, 19–20 cm. However, separate chemical analyses, including pyrolysis mass spectral analysis, were run on this sample. It was extracted with methylene chloride/methanol (90:10); the solvent was evaporated, replaced with hexane, and separated into saturate aromatic and NSO (nitrogen, sulfur, oxygen) compounds/resins by liquid chromatography (LC). The LC separation used a Whatman Partisil PAC Magnum 9 column. LC conditions were: sample—150 μl by sample loop; primary solvent—hexane, secondary solvent—methylene chloride; program—8-minute delay, 8-minute linear solvent gradient; pumping rate—5 ml/minute; temperature—50°C. Gas chromatography (GC) was performed on a Hewlett Packard 5710-A with a 30-m fused silica DB-1 bonded phase-capillary column (J&W Scientific), temperature-programmed from 130 to 300°C at 4°/minute. Gas chromatography/mass spectrometry (GC/MS) was performed with a Hewlett Packard 5985A instrument using the same GC column and conditions.

## LITHOLOGY, PETROLOGY, AND ORGANIC GEOCHEMISTRY

For purposes of summary and discussion, it is convenient to consider both the "inorganic petrography"—texture, mineralogy, and inorganic depositional constituents—and the "organic petrography"—organic geochemistry and kerogen characteristics of these rocks—together in this section.

Figures 4 and 5 indicate the stratigraphic positions of the samples, from Sites 535 and 540, and summarize many of their organic-geochemical and petrographic characteristics. Table 1 summarizes the stratigraphic position of the one sample (Eocene) from Hole 538A. Figure 6 shows van Krevelen diagrams, including the approximate position of the isovitrinite reflectance ($R_o$) line for $R_o$ = 0.5. Figure 7 shows the percentages of paraffins, naphthenes, and aromatics in the pyrolyzed hydrocarbons, and Figure 8 summarizes the compositions of the naphthene fractions in terms of monocyclic, dicyclic, and larger molecules.

Table 1 summarizes the descriptive inorganic petrography of the samples grouped by age, lithologic unit, and lithology. Appendix D summarizes the compositions of the samples in terms of organic constituents (kerogen, from residue slides) and inorganic constituents (grain types, from thin sections). Appendix E presents semiquantitative mineralogic compositions determined by X-ray diffraction analysis. The core photographs and thin-section photomicrographs in Plates 1–5 illustrate the lithologic characteristics of the carbonates.

### Berriasian and Early Valanginian (Site 535, Unit V)

The samples from this unit, Sample 26 from the late Berriasian and Samples 22–25 from the early Valanginian, are relatively light-colored lime mudstones composed of alternating light olive gray (5Y 7/1-6/1) and medium-to-dark olive gray (5Y 4/1-3/1), planar-parallel laminations up to a few millimeters in thickness (see Plates 1 and 2). Lighter-colored laminations, commonly bioturbated and apparently impoverished in organic matter, predominate in the older, deeper samples (23–26), and darker, more planar and somewhat better defined laminations predominate in the youngest sample. The trend upwards to darker and more evenly laminated lithologies continues through Samples 17–21 from the Valanginian part of Unit IV, which will be discussed under the next heading. Comparisons between these two groups of carbonates in terms of "darkness" and character of laminations can be made in Plate 1.

These rocks are characterized by relatively high carbonate contents of 47–63% (calculated as $CaCO_3$); as much as a few percent silt-size terrigenous grains (quartz); traces of calcispheres and phosphatic grains; highly elongate, spindle-shaped, apparently compacted entities interpreted as former soft pellets (discussed in a later section); and anywhere from a few percent to 20% dolomite. Dolomite occurs as disseminated rhombs or in spindle-shaped, augenlike clusters of rhombs replacing former burrow fillings. Planktonic foraminifers are very rare or absent from these carbonates and in fact from most of the Neocomian carbonates in Hole 535 (Berriasian-Hauterivian).

The organic fractions of these lime mudstones are quite consistent, with moderately high total organic carbon (TOC) contents of 1.1–2.2% (Fig. 4) and kerogen fractions composed of mostly amorphous matter (marine) and some terrestrial matter (fusinite and vitrinite). In Sample 26 spores are fairly common. By pyrolysis, these samples yielded relatively high oxygen indexes (OI) and therefore plot on a van Krevelen diagram (Fig. 6) very close to the line for Type III organic matter and appear to be dominantly gas prone. Their pyrolyzed hydrocarbons are poorer in aromatics (see Fig. 7) than those from most other samples, probably indicating the general lack of preservation caused by oxidizing conditions. This is consistent with the lack of laminations, and bioturbation is suggested by low RI values (except for Sample 25, see Appendix C). The presence of a significant terrestrial organic-matter fraction is also suggested by

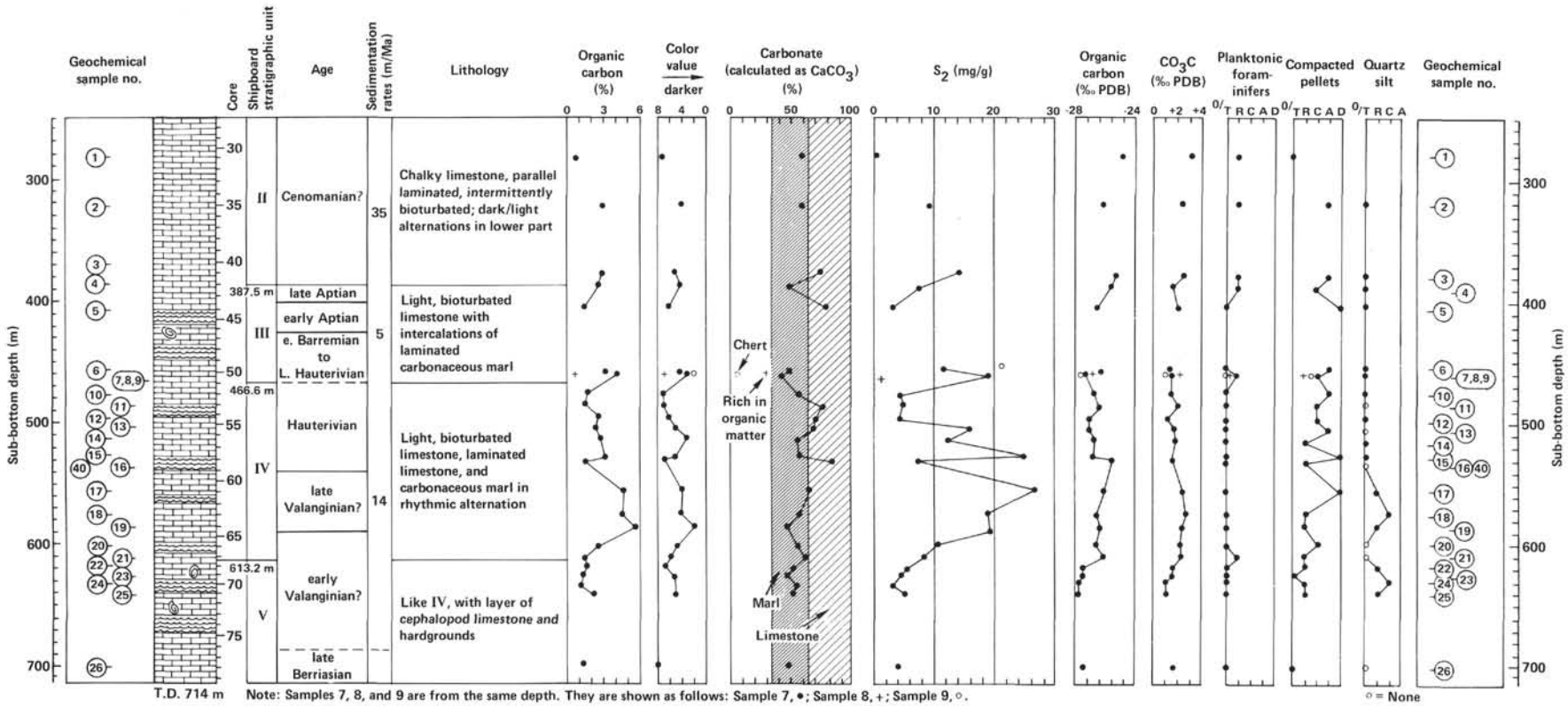


Note: Samples 7, 8, and 9 are from the same depth. They are shown as follows: Sample 7, ●; Sample 8, +; Sample 9, ○.

Figure 4. Stratigraphic summary chart for sampled portion of Hole 535. Age interpretations and lithologic column are from Buffler and others, this volume; lithology descriptions are from shipboard volume. Other symbols and approximate percentages: Sample 7 = ●, 8 = +, and 9 = ○; T = trace (0–1%); R = rare (2–4%); C = common (5–10%), A = abundant (11–20%), D = dominant (>20%); T.D. = terminal depth. Color value scale is after GSA Rock-Color Chart; hues of samples are dominantly 5Y.

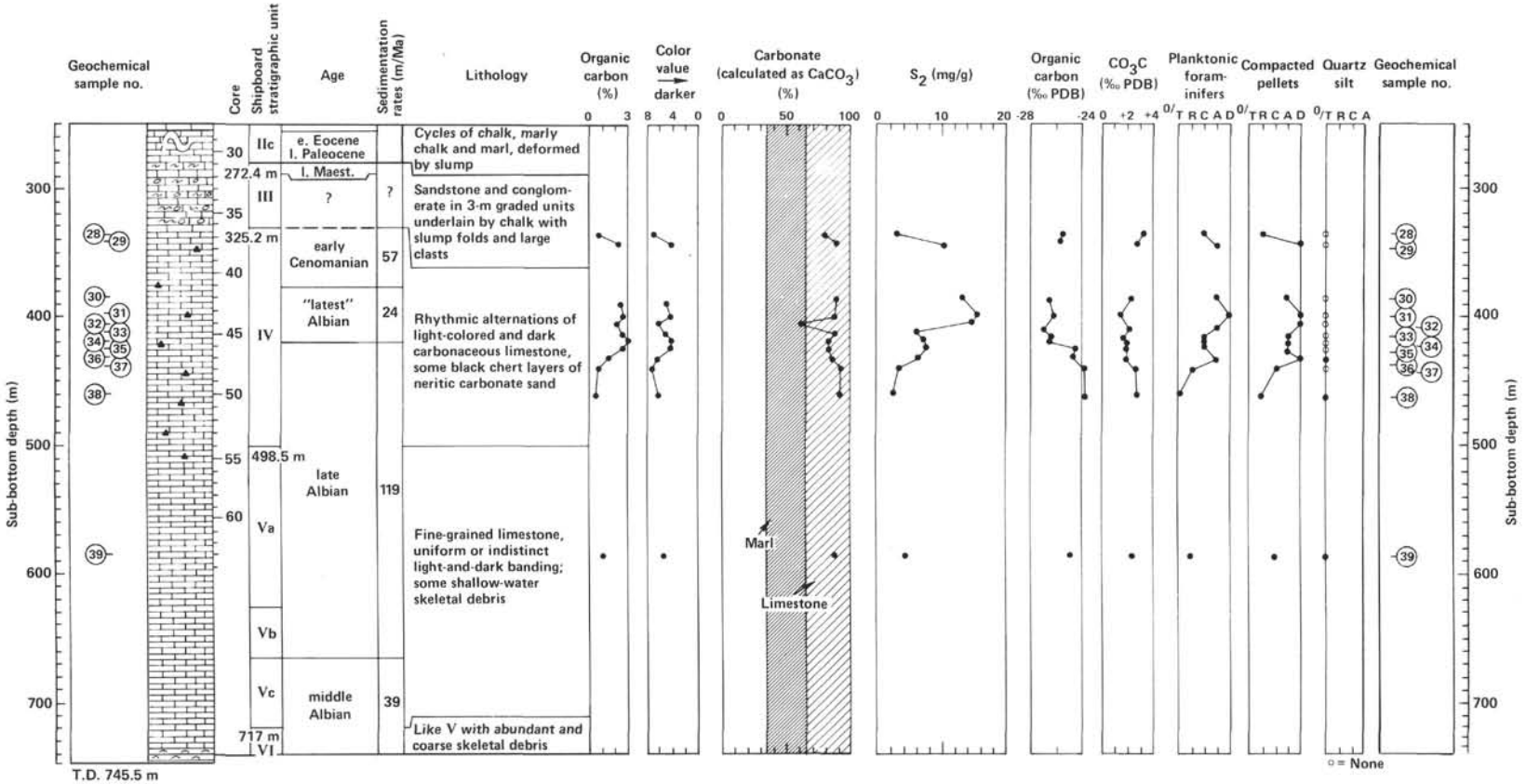


Figure 5. Stratigraphic summary chart for sampled portion of Hole 540. See Fig. 4 caption for further explanation.

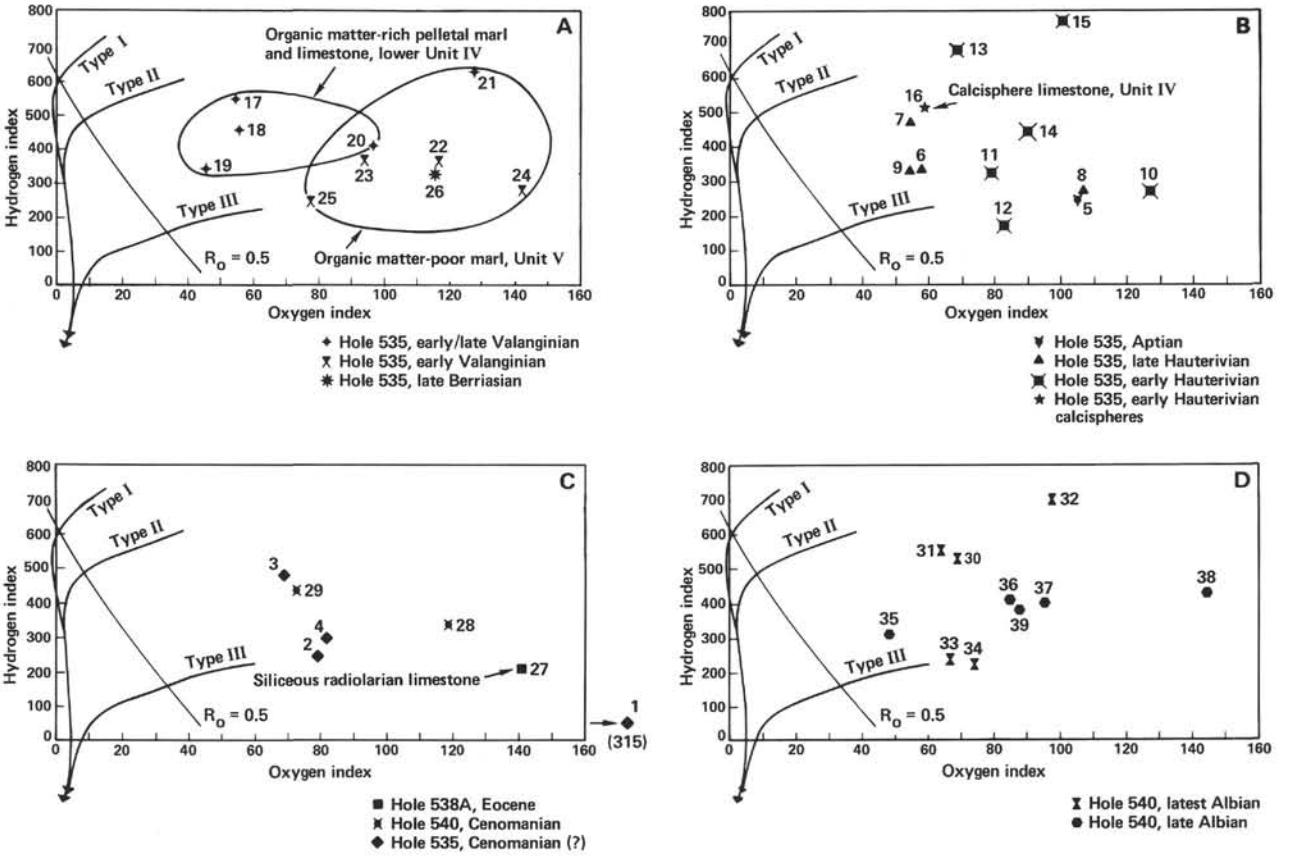


Figure 6. Hydrogen and oxygen indexes, for samples studied as grouped by biostratigraphic age, plotted on a van Krevelen diagram. Lithostratigraphic units, lithologies, and organic richness of most samples are indicated on Figs. 4 and 5. A. Late Berriasian to late Valanginian cemented marls (mostly lime mudstones) from Hole 535. Samples 17–20 are darker colored, more organic-carbon rich, and richer in compacted pellets than Samples 21–26. B. Early Hauterivian to Aptian limestones and marls of varied compositions (see Fig. 4 and Table 1) from Hole 535. C. Cenomanian limestones and marls (lime mudstones) from Holes 535 and 540, and an Eocene siliceous lime wackestone with radiolarians from Hole 538A (Sample 27). Hydrogen index varies directly and oxygen index inversely with organic carbon content and darker color (see Figs. 4 and 5). D. Albian limestones from Hole 540. Samples 35–38 are laminated wackestone-packestones with sparser planktonic foraminifers than Samples 30–34 (mudstones), and are lighter colored and less organic-carbon rich.

relatively light values of organic-carbon $\delta^{13}C$ and a relative abundance of terrigenous silt (Fig. 4).

### Valanginian (Site 535, lower half of Unit IV)

Samples from this sequence, Samples 17–21, are similar to Sample 22 in their relatively dark color but have considerably better-defined, planar-parallel laminations and common to dominant compacted pellets (Appendix D). Like Samples 22–26 they are mostly lime mudstones containing a few percent silt-size quartz grains of terrigenous origin, traces of calcisphere and phosphatic grains, and dolomite in trace or minor amounts, with no planktonic foraminifers. X-ray diffraction analysis reveals the presence of trace amounts of illite. Carbonate contents calculated as $CaCO_3$ are 48–67%, essentially the same as those just cited.

These late Valanginian carbonates contain as a group more abundant organic matter than any other of our samples from Site 535, 4.1–5.5% TOC. The general ratio of terrestrial organic matter (chiefly fusinite, vitrinite, and pyrobitumen; see Appendix D) to marine amorphous kerogen is about the same, and the amorphous kerogen is more abundant than in Samples 22–26. This mix of kerogen types is clearly seen by the bimodal distribution of the cracking region in the orthographic pyrolysis plot of Sample 19 (Fig. 2C).

Hydrogen indices (HI) tend to be higher and OIs lower, however, so that these samples plot closer to the evolutionary trend for Type II kerogen (Fig. 6). In a general way there is an upward change in these Valanginian and Berriasian carbonates toward more organic matter–rich, darker, more evenly laminated, and presumably more anoxic lithologies; core Samples 18–26 illustrate this change (see examples in Plate 1). Accompanying it is an upward tendency toward more hydrogen-rich and therefore more oil-prone kerogen (Fig. 6), toward less paraffinic and more aromatic rich hydrocarbons (Fig. 7), and toward naphthenes that are more dominated by tricyclics (Fig. 8). The upward shift seen toward heavier organic-carbon $\delta^{13}C$ suggests that the kerogen becomes more marine in makeup (see Fig. 4, Samples 18–26).

For the Valanginian group, Samples 17–21, the pyrolysis mass spectral data (see Appendix B) also support the interpretation of a more oil-prone kerogen, in an anoxic depositional environment resulting in a good to very good oil-source potential assignment.

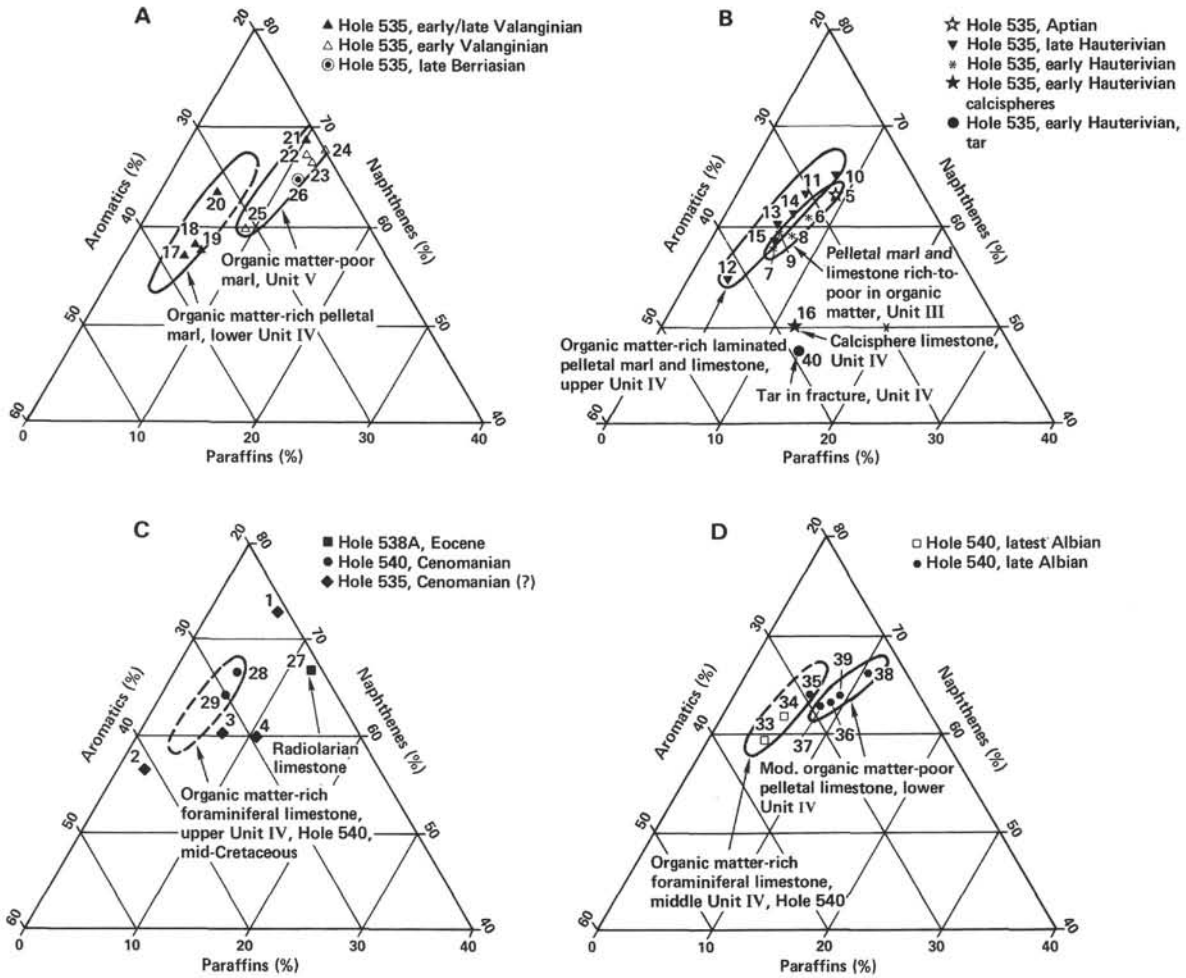


Figure 7. Triangular diagrams showing percentages of paraffins, naphthenes, and aromatics (PNA) in the pyrolyzed hydrocarbons from study samples, calculated from data from 300–600°C. Composition of tar from fractures in Section 535-58-4 (Sample 40) is shown in B. Principal lithostratigraphic units have generally distinct PNA compositions. Most samples of dark, well-laminated, anoxic lithologies, especially Units IV of Holes 535 and 540, are enriched in naphthenes and impoverished in paraffins compared to others. The term "organic matter-poor" is used in a relative sense for this study only; the samples are not poor in organic matter in the usual sense. (See caption to Fig. 6 for comments on petrography.) A. Late Berriasian to late Valanginian laminated marls. B. Early Hauterivian to Aptian limestones and marls. Sample 40 is tar from a fracture in marl from Unit IV near the site of Sample 16. C. Cenomanian limestones and marls from Holes 535 and 540, and an Eocene siliceous limestone from Hole 538A. D. Albian limestones from Hole 540.

## Early Hauterivian (Site 535, upper half of Unit IV)

Samples 10–16 are from the Hauterivian part of Unit IV. Sample 16 is unique among the entire suite of Leg 77 samples we studied in containing an abundance (up to about 20%) of probable calcispheres (Fig. 2; Plate 3, Figs. 5–6; Appendix D). This lime mudstone–wackestone (86% $CaCO_3$) shows signs of mild compaction in the form of shreds of organic matter draped or deflected over the rigid, calcite-filled calcispheres (see discussion in a later section). But compacted pellets are lacking altogether, as are planktonic foraminifers.

Sample 16 also is distinctive geochemically, with an organic-carbon $\delta^{13}C$ less negative and more marine than those of any other carbonates from Units IV and V (−26‰, Fig. 4). But the TOC of this sample is relatively low, around 1.5%. The close similarity in PNA (Fig. 7) between Sample 16 and the tar (Sample 40) found stratigraphically near it suggests that the hydrocarbons pyrolyzed in Sample 16 may be migrated rather than indigenous. However, the amorphous material in Sample 16 is unique in the entire suite of samples in that it consists of distinctive yellow clumps that have more body than the more usual fluffy type of amorphous matter. This amorphous kerogen is reminiscent of the oil-generating alga *Botryococcus,* a green alga (Chlorophyceae). The calcispheres are believed to be calcified spores of dasycladacean algae, which are also green algae (Chlorophyceae), and therefore we suspect that this particular type of amorphous matter may be derived from green algae (see later discussion).

The low RI (1.10) for Sample 16 suggests an oxic depositional environment; that, coupled with a relatively high PPI (~22.4%), supports the view that much of this material has migrated into the interval.

The other samples from this Hauterivian part of Unit IV, Samples 10–15, are lime mudstones and wackestones similar in general to the older samples from Unit IV,

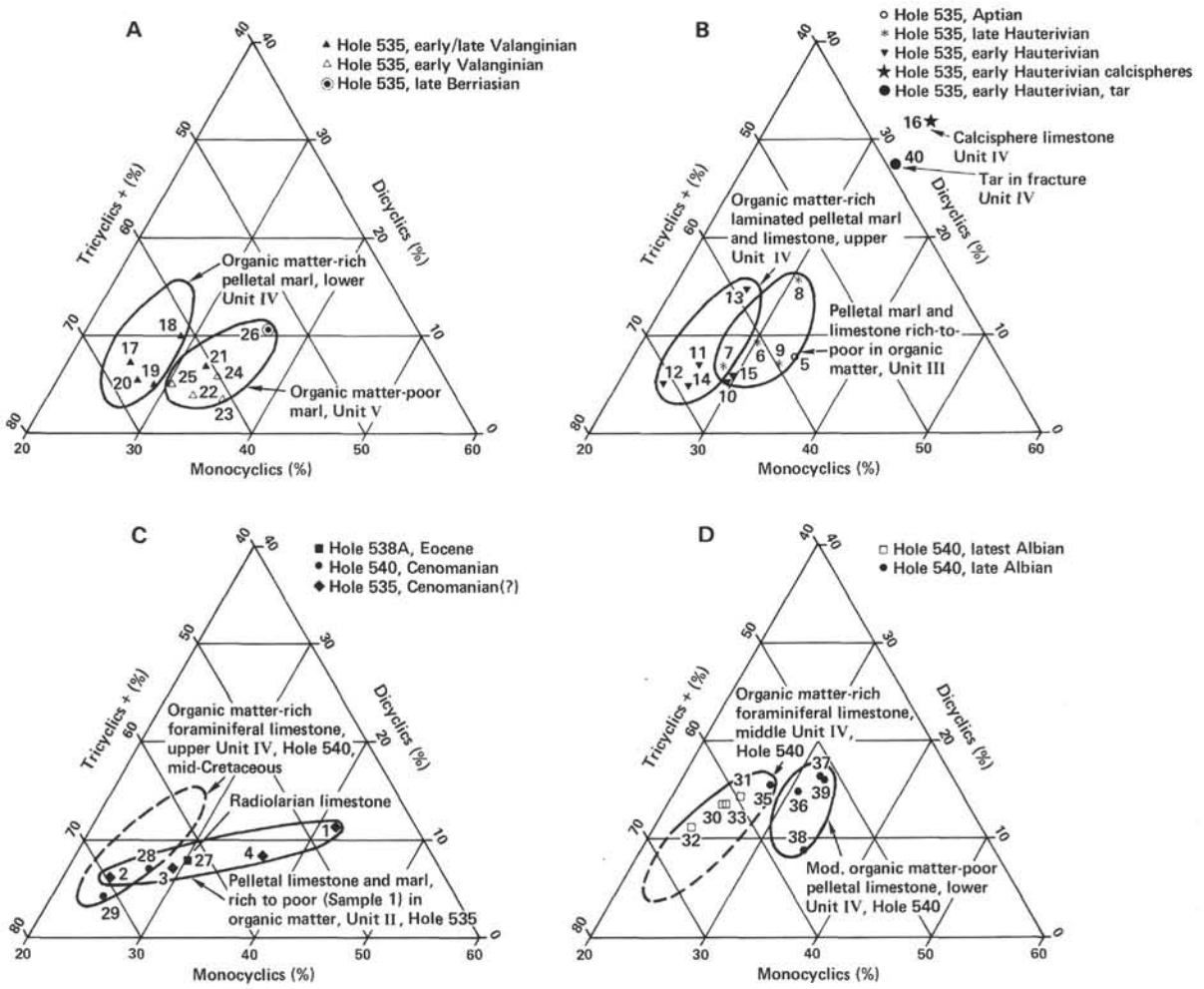


Figure 8. Triangular diagrams showing percentages of monocyclic, dicyclic, and tricyclic or greater components in naphthenes from the pyrolyzed hydrocarbons, 300–600°C. Composition of tar from fractures in Section 535-58-4 (Sample 40) is shown in B. See Figure 7 caption regarding the terminology "organic matter-poor." (See Fig. 6 caption for petrography comments and descriptions of A–D.)

Samples 17–21 (see Plate 1): they have well-defined planar-parallel laminations; dark to moderately light-colored laminae (5Y 2/1–5Y 6/1); rare to common (trace to 15%) dolomite in the form of scattered rhombs and dolomitized burrow fillings or pellets (Plate 4, Figs. 1–2) and very conspicuous, abundant compacted pellets (Plate 3, Figs. 3–4). Total carbonate, calculated as $CaCO_3$, is 55–77%, somewhat more than in the rest of Unit IV; the remaining, noncarbonate fractions are composed of terrigenous silt, organic matter, and illitic clay.

These carbonates are a little less rich (1.5–3.1%) in TOC than Sample 17–21. Their kerogen fractions visually resemble those of the rest of Unit IV but are somewhat less rich in tricyclic naphthenes (Fig. 8), aromatics (Fig. 7), and hydrogen (Fig. 6), suggesting that they have been less oxidized and are more oil prone. The relatively paraffinic nature of the pryolysate from Sample 10 may be a reflection of the spores and cuticle found in that sample (Appendix D).

Viewed as a whole, Samples 10–21 from Unit IV at Site 535, a unit that is split about 50:50 between the Valanginian and Hauterivian, are distinguished by very well-developed planar-parallel laminations, an abundance of compacted pellets, an absence of planktonic foraminifers, scattered calcispheres (abundant in Sample 16), and dolomitized pellets. The dark colors and laminar structure suggest that anoxia prevailed during the accumulation of Unit IV, particularly the Cenomanian portion. On a van Krevelen diagram (Fig. 7), all of the samples plot in a well-defined region that coincides with that for Samples 22–26 from Unit V and suggests by its position that the kerogen in these carbonates is immature. Moreover, the amorphous kerogen fraction is mostly clumps, filmy or membraneous, suggesting a fecal origin. This is reasonable, in light of the abundant pellets in Unit IV. The pellets are less abundant and the kerogen is less strongly skewed toward Type III (Fig. 6) in the samples from Unit V.

### Late Hauterivian–Early Barremian (Site 535, bottom Unit III)

Samples 6–9 from this unit provide a small scale sampling interval because they all came from basically two sections in a single core from Site 535 (535-50-2 and 535-50-3). Samples 6 and 7 are lime mudstone–wackestone with 41–48% equivalent $CaCO_3$, sparse plankton-

ic foraminifers, and rare to abundant compacted burrows; Sample 8 is chert (Plate 4, Figs. 5–6) with only 3% $CaCO_3$; and Sample 9 is very organic rich mudstone-wackestone with only 29% $CaCO_3$.

Organic matter is very abundant in Samples 6, 7, and 9 – 3.5, 4.0, and 6.6% respectively. Amorphous marine kerogen appears to be dominant. The low OI values and high RI values (5.6–15.5) for Samples 6, 7, and 9 suggest anoxic and oil-prone conditions. Sample 8, the chert (Plate 3, Figs. 5–6, Appendix C), has distinctly more oxidized kerogen (Fig. 6). The RI value of 1.1 suggests an oxidizing environment.

**Aptian (Site 535, upper part of Unit III)**

Only one sample, Sample 5, was collected from the Aptian part of Unit III. It is basically similar to Samples 6 and 7 but contains more abundant compacted pellets (Plate 4, Figs. 3–4), has a lower TOC (1.3%), and contains somewhat less amorphous kerogen. Also, its kerogen shows considerably more evidence of oxidation (Fig. 6). Here, the RI of 1.5 strongly supports the interpretation of oxic depositional and/or early diagenetic conditions.

**Albian (Site 540, Units V and IV)**

Sample 39 is from Core 540-63, depth 584.9 m, in the upper part of Unit V. It differs from the Early Cretaceous carbonates sampled in Hole 535 in having only slight traces of terrigenous silt. Otherwise its sedimentologic characteristics are similar, including the presence of compacted pellets.

Samples 30–38 differ significantly from any of the pre-Albian sediments from Hole 535. With the exception of Samples 30 and 31, these carbonates are less distinctly laminated that the older Cretaceous carbonates. Also (cf. Figs. 4 and 5), these Albian carbonates from Cores 540-42 through 540-50 are true limestones with 80–95% equivalent $CaCO_3$, whereas most of the Early Cretaceous carbonates are in fact marls. (Sample 32 with only 61% $CaCO_3$ contains internal chambers of planktonic foraminifers filled with chalcedonic quartz.) Moreover, the Albian limestones contain little or no terrigenous silt and significant quantities of planktonic (globigerinid?) foraminifers (e.g., Plate 5, Figs. 2–3). Compacted pellets are omnipresent in these pelagic limestones, commonly in such abundance that they give the fabrics of the limestones a "welded" appearance. Foraminifers tend to be more concentrated in laminae rather than distributed uniformly.

The organic fractions of these late Albian limestones also are distinctive. TOC's are relatively low to moderate in Samples 36–38 (0.6–1.6%), as expected from their relatively light colors, and are higher in Samples 30–35 (2.1–3.2%), which are darker carbonates (Fig. 5 and Plate 2). The stratigraphically lower group (Samples 36–38) has fewer planktonic foraminifers and less amorphous kerogen than Samples 30–35.

The organic geochemistry of these samples substantiates these conclusions. Samples 36–38 show low RI values, 0.8–2.0, indicating oxidizing conditions. Pyrolysis mass spectral data and Rock-Eval data also suggest a marine oil-prone material deposited in an oxidizing environment.

The organic $\delta^{13}C$ values for these samples are among the heaviest seen among Leg 77 samples (−24.7 to −23.9‰), which firmly supports their more marine character.

Samples 30–35 show more anoxic conditions (RI values from 3.0 to 6.9) and hence better preservation of the organic matter. The $\delta^{13}C$ values (−27.0 to −24.5‰) suggest an admixture of marine and terrestrial material. The pyrolysis mass spectral and Rock-Eval data support a more anoxic depositional environment and an improvement in the source potential.

On a PNA diagram (Fig. 7) all the Albian limestones lie in the central part of the general trend for most of the samples. But on a naphthene-composition diagram (Fig. 8) they lie along a distinct trend of their own, being richer in dicyclics than most other samples. Sample 38, the exception to this, contains much less amorphous kerogen and contains some dinoflagellate kerogen, which may explain its anomalous naphthene composition.

**Early Cenomanian (Site 540, Unit IV)**

Two samples, 28 and 29, were collected from Core 540-37 near the top of Unit IV. Petrographically and geochemically Sample 29 closely resembles the late Albian foraminiferal limestones just described, but Sample 28 differs in having about 15% chalcedonic quartz filling what seem to be molds of radiolarians or diatoms and in containing much fewer pellets. Graded laminations about 0.5 cm thick, composed of very fine sand-size carbonate grading upward to micrite suggest thin distal turbidites.

**Cenomanian(?) (Site 535, Unit II)**

The four samples from Unit II at Site 535, Samples 1–4 (see Appendixes D and E) have varying petrographic characteristics and kerogen compositions. They are mostly marls with no detectable terrigenous silt but appreciable amounts of illite and quartz by X-ray diffraction analysis; lots of compacted pellets; and very few foraminifers. Petrographically they closely resemble Samples 37–39 from the Albian at Site 540, suggesting that parts of Unit II at Site 535 may in fact be Albian.

The organic compositions tell a different story, however, and differ somewhat from those of the Albian pelagic limestones. Samples 2–4 are clearly different, and Sample 1 is a unique among all other carbonates we studied. Sample 1, with its light color, exceptionally high OI (315), and RI of only 0.8, clearly represents oxidizing bottom conditions; its TOC is only 0.7%, the lowest of any of our carbonates, and it is comparatively rich in monocyclic naphthenes. Samples 2 and 3 are unexceptional generally. Sample 4 is different, containing no fecal amorphous matter but substantial amounts of dinoflagellate material, which may explain its relative depletion in naphthenes compared with most other samples.

**Late Eocene (Hole 538A, Unit II)**

A single sample from Hole 538A was analyzed, Sample 27 from sub-bottom depth 141.8 m and from an interval in Unit II dated by nannofossils as late Eocene. It

is described (Schlager et al., in press) as "nannofossil ooze, nannofossil chalk, radiolarian-nannofossil chalk, (and) minor volcanic ash?"

Viewed with a petrographic microscope, Sample 27 (Sample 538A-16-5, 21–27 cm) is a medium-light olive gray (5Y 5/1) siliceous limestone, with about 5% radiolarians, the tests of which have been partially to completely dissolved and the resulting molds filled by chalcedonic quartz. Planktonic foraminifers, empty of material except for submicron-size opaque granules of sulfide(?), make up a few percent. Considerable compaction of the lime-mud matrix is inferred from wispy bits of organic matter deflected around or draped over rigid grains; however, radiolarians and foraminifers are uncrushed. Carbonate content is 48% (equivalent $CaCO_3$).

Like all the other carbonates in this study suite, the Eocene radiolarian-rich, siliceous limestone contains abundant terrestrial organic matter, along with abundant amorphous matter and some dinoflagellate material. The TOC is fairly high, 2.5%, but the organic fraction has been strongly oxidized and is clearly gas prone (Fig. 6). The pyrolyzed hydrocarbons are enriched in paraffins (Fig. 7), but their naphthenes are not especially distinctive compositionally (Fig. 8). The RI of 1.54 supports oxidized organic matter, and the $\delta^{13}C$ supports a dominantly marine source.

## NATURE AND MATURATION OF KEROGEN

The kerogen fractions in these materials were studied by a technique known as visual kerogen analysis (VKA). In this technique, the rock material is dissolved (macerated) with hydrofluoric and hydrochloric acids, and the remaining organic residue is examined on slides with an optical microscope, at magnifications of $\times 500$ and $\times 1000$. In this study, degree of maturity was estimated from the color in transmitted light of the spore and cuticle fractions of the kerogen observed in the macerals.

### Characteristics of Kerogen

The types of kerogen observed in these carbonates are summarized in Appendix D. Fusinite, vitrinite, and pyrobitumen are terrestrial kerogens considered to be gas prone. Fusinite is charcoal, oxidized wood. Vitrinite is wood that has undergone maturation but has retained its morphology and is recognizable as wood. "Pyrobitumen" is used here, for lack of a better term, for carbonized or oxidized organic matter that clearly is not wood, but rather is opaque, lacks the linearity and angularity of wood tissue, and shows no internal anatomy; it simply is nonwoody organic matter charred into lumps. All of these gas-prone kerogens are conspicuous in virtually all of the samples.

Other kerogens, regarded by us as terrestrial (Appendix D), include spores, cuticle, fungal spores, and/or hyphae; however, these types are considered to be oil prone, along with all of the kerogen we classify as "amorphous."

### Kerogen Maturation

Although spores (pollen) are sparse in these samples as is plant cuticle, these are the two kerogen types conventionally used to estimate maturation by color changes. In this particular sequence, the estimates of maturation based on these two kerogen types are questionable for two reasons. First, the light brown or tan color of the spore-cuticle fraction, classified as 5− on our scale from 1 to 10 (2+ on conventional scale), persists from the oldest to the youngest samples; we would expect to see at least a slight darkening with depth within a sequence represented by our samples of about 550 m and an age range of some 40 Ma. Second, most of the spores that yielded the 5− color are grains of *Classopolis,* a genus associated with the Jurassic, though ranging through Early Cretaceous time. These considerations suggest that the light brown spores may have been reworked from Jurassic rocks. If the spores in Sample 26 (our oldest sample), which are orange yellow in color and 4 on our scale (2 on the conventional scale), are indigenous, then all the other samples, because they are younger, should be less mature. A thermal alteration index (TAI) of 4 (our scale) is roughly equivalent to 0.6% on the vitrinite reflectance scale.

Conventional interpretation is that oil generation starts at a maturation level of 0.5–0.6% reflectance, the top of the oil window. If this interpretation is valid here, then Sample 26 is either on the verge of entering the oil window or is just barely inside it, and everything above this stratigraphic level (Berriasian) at Site 535, and presumably Site 540, must be thermally immature. This conclusion is consistent with the interpretation of thermal immaturity that is based on the van Krevelen diagram of Figure 6.

## MINERALOGY OF THE CARBONATES

X-ray diffraction analysis of a reconnaisance nature was done on all 39 rock samples. The samples were first crushed and ground to finer-than-44 $\mu$m particle size, but there was no other preparatory treatment. The results are summarized in qualitative-semiquantitative form in Appendix E. Although they must be regarded as preliminary, they do reveal features not discerned in the thin sections and merit some discussion here.

As noted in Appendix E, constituents identified there as dolomite were identified in a number of thin sections, notably those from the Lower Cretaceous, Berriasian through Hauterivian fine-grained carbonates (Units III–V) in Hole 535. X-ray diffraction analysis of these samples indicates that the "dolomite" is of varying mineralogy. From d-spacing reflections alone, three double carbonates were identified; (1) Mg-kutnahorite (a dolomite-like carbonate in which $Mn^{+2}$ substitutes for about half the Mg), (2) dolomite, and (3) "ankerite" or ferroan dolomite (listed as "ankerite" in Appendix E). The occurrences and distributions of these carbonate minerals are not greatly different from one another, suggesting that the differences between them are not as sharp as the listing implies. For example, the dolomite in Sample 11 (Plate 4, Figs. 1–2) visually resembles quite closely the "ankerite" in Samples 18 and 26. More likely, what we are seeing is a range of metal-ion compositions in the double carbonates, in response to variation in pore-water composition, composition of the organic fractions,

degree of redox conditions, or some combination of these factors. That a continuum may be represented is further suggested by the difficulty experienced in interpreting the double-carbonate mineralogy of many of these samples; the array or reflections they show commonly fits poorly with the "standard" reflections of all three minerals mentioned.

An exception is seen in the occurrences of ankerite or ferroan dolomite in Samples 28–30 and 34–36, where the mineral is found specifically filling or lining the interiors of globigerinid tests. Double carbonates with this type of occurrence are very commonly ferroan in many other carbonate sequences and undoubtedly record iron-rich and/or strongly reducing microenvironments induced by decaying organic matter.

Also of note in the X-ray data are the common occurrences of gypsum, generally in trace amounts. Gypsum was not identified in the "matrices" of our samples, but was found (once its presence was suspected) quite commonly in what appear to be fractures. Its mode of occurrence suggests that it is not indigenous to these carbonates, but may instead have precipitated from evaporating pore waters after recovery of the cores.

The occurrence of kaolinite also is noteworthy. Except for a doubtful trace in Sample 1, kaolinite is entirely restricted to Samples 17–26, the Berriasian-Valanginian sequence at Site 535. This same sequence also contains a relative abundance of detrital (clastic) quartz silt, and we suspect that the kaolinite in these samples, which was not detected in thin sections, is probably of terrigenous origin rather than diagenetic.

## SPECIAL PETROGRAPHIC FEATURES

A number of features appear to have significance in interpreting the organic-geochemical characteristics and the organic-inorganic diagenesis of these carbonates. These features include: (1) the calcispheres abundant in Sample 16; (2) the abundant, nearly ubiquitous entities interpreted as compacted soft (fecal?) pellets; (3) the abundant evidence of mechanical compaction in nearly all these marls and limestones; and (4) the characteristics of cements visible with a petrographic microscope. We have not done special studies of these materials with a scanning electron microscope or microprobe, nor have we attempted isotopic or minor-element geochemical studies of the dolomite or other special fractions of these rocks.

### Calcispheres

As noted earlier, calcispheres are abundant in one sample (Sample 16) from the Hauterivian part of Unit IV in Hole 535 (Fig. 4 and Plate 3, Figs. 5–6). Whether coincidentally or not, the amorphous material in this particular sample is unique in the entire suite of rocks, and certain other properties such as the organic-carbon $\delta^{13}C$ are also distinctive. We have already alluded to the amorphous kerogen.

Calcispheres are poorly understood, but in recent years there has been a growing concensus (e.g., Rupp, 1967; Wray, 1977; Marszalek, 1975; Bein and Reiss, 1976) that they are probably reproductive parts of benthic green algae. Marszalek (1975) described the calcisphere-producing alga *Acetasbularia* in shallow, sheltered marine shelf environments in the Florida Keys. Bein and Reis (1976) described the calcisphere *Pithonella* from Mid-Cretaceous limestones of the Mount Carmel area in Israel and concluded that these 100-$\mu$m spherical bodies were free-floating oogonia(?) of a benthic alga that populated outer-shelf environments.

There appears to be a close similarity between the amorphous kerogen found in Sample 16 and the remains of *Botryococcus,* also an alga. Thus these cumulative observations and interpretations suggest that: (1) the calcispheres are in fact of algal origin, and (2) the amorphous material in Sample 16 is algal.

But the calcispheres in Sample 16 now are completely filled by microspar calcite; their internal soft material has been expelled (possibly via the circular opening in each algal cyst) and completely supplanted by inorganic cement. Where did the soft material go?

The character of the kerogen suggests that the internal fillings in the calcispheres, though chemically altered, have remained at least in part within this lime mudstone-wackestone. Presumably the kerogen derived from them is entrapped in the micritic matrix of the rock.

### Compacted Pellets

Present in essentially all of these carbonates, in amounts up to 60–65% (estimate), are micritic grains and other entities provisionally interpreted as pellets (Appendix D). In a few samples (e.g., Sample 35) these constituents are elliptical or oval in shape and clearly resemble pellets of fecal origin; dimensions of 20–35 $\mu$m width and up to 100 $\mu$m length are typical. More usual are highly elongate "grains" with length-to-width ratios well in excess of 10, widths of approximately 10–15 $\mu$m and lengths up to 0.8–0.9 mm, and shapes that vary from distinctly spindle-shaped or augen-shaped with attenuated ends to simply "tubular." Where shapes are this highly elongate, it is difficult to be certain what the original constituents were. However, the most elongate shapes are associated with various other features that suggest intense mechanical compaction and stratigraphic "shortening." These features include: (1) draping and thinning of the micritic entities over obviously rigid grains such as foraminifers and other skeletal fragments; (2) similar deflection of organic shreds around grains; (3) merging of the elongate micritic entities; and (4) strong preferred orientation parallel to the plane of stratification. The lack of bifurcation or orientation at angles to stratification also further indicate the nature of these micritic constituents.

Taken together, these features are interpreted to mean that the micritic constituents are in all likelihood formerly soft pellets, probably of fecal origin. Because the carbonates containing these pellets have such seemingly undisturbed laminations, the pellets cannot have been produced by infauna or epifauna. More likely they are products of swimmers in the overlying water column.

### Cementation and Compaction Features

Essentially the only cementation likely in these carbonates involved the micrite-rich, lime-mud, and compacted-pellet "matrix," which at best is partly indurated. Larger pore spaces such as the chambers of foraminiferal tests in general contain little or no carbonate pore-filling cement; what little cement there is occurs as minutely thin fringes on the order of a micron thick, composed of $CaCO_3$ as determined with alizarin red stain and calcite as inferred from stubby crystal forms.

Despite the compaction, foraminiferal tests and other fragile bioclastic grains rarely show breakage effects. Rather, it is apparent that mechanical compaction has been confined almost entirely to the soft pellets and lime-mud fractions. By inference, partial cementation also has occurred preferentially in those fractions.

Compaction has had at least two consequences that can be observed visually. One is the creation, in effect of "diagenetic" mudstones and wackestones from sediments that in some cases probably were packstones and grainstones initially. Plate 3, Figures 3–4, and Plate 4, Figures 3–4, illustrate fabrics of this kind. Other carbonates that now are mudstones and wackestones probably were such initially, as illustrated by the photomicrographs in Plate 3. Another visual effect of mechanical compaction is the creation of pseudolamination caused by rotation and squashing of soft pellets and by squeezing and smearing out of soft organic material. The resulting fabric has a streaky, laminar appearance but does not show graded bedding or other vertical changes in grain size or grain-to-matrix ratios. Among the carbonates of this type are Samples 2, 3, and 6. More commonly, the rocks exhibit both true sedimentary lamination and overprinted compaction effects that accentuate the primary structure.

Although these highly compacted carbonate sediments are not very deeply buried under sediment overburden, the combined load of both a sediment column of approximately 300–700 m present (postcompaction) thickness and an overlying water column approximating 3000–3500 m (Schlager et al., in press) is more than sufficient to have induced intense compaction. Experimental work by Shinn and his associates (Shinn et al., 1977; Shinn and Robbin, in press) produced significant compaction at simulated hydrostatic burial depths of less than 333 m, and somewhat earlier experimental work by Fruth and others (1966) also produced very strong early burial compaction effects under load pressures of less than 100 bars, equivalent to about 500 m of sediment. From the results of this experimental work and other lines of evidence, it seems reasonable to infer that these sediments that appear highly compacted are buried at perhaps no more than one-half their original burial depths, and that their mobile organic matter and derivatives are at least in process of being expelled as a result of mechanical compaction.

## TAR/ASPHALT FROM SITE 535

Sample 40 is the tar/asphalt sample from Sample 535-58-4, 19–20 cm. This material was separated by liquid chromatography so that the saturate fraction could be analyzed by GC and GC/MS.

Carbon isotope data have been obtained for both the whole sample and the various cuts obtained by liquid chromatography. All values are reported versus PDB as a standard: whole sample, −25.63‰; saturates, −26.47‰; aromatics, −25.80‰; NSO/resins, −26‰. These values are not out of the ordinary. Aromatics are usually more positive than the saturates, and the overall range of values is reasonable for mixed material of a mixed marine/terrestrial origin.

More interesting data have been obtained through GC of the tar sample (Fig. 9). Approximate *n*-paraffin carbon numbers are shown and demonstrate that paraffins can just be seen above the naphthene envelope below about $C_{25}$. This clearly supports biodegradation of this material. However, the peaks seen above about $C_{25}$ are not due to paraffins; instead they represent triterpanes and steranes.

Even more interesting data were obtained by GC/MS. Figure 10A shows the mass fragmentogram for m/e = 191; Figure 10B shows the total ionization in the selective ion monitoring mode for m/e = 57, 191, and 217; Figure 11A shows the mass fragmentogram for m/e = 217. These are diagnostic for the triterpanes and steranes respectively. The carbon numbers of some of the main peaks and three important steranes (II, III, and IV, see next paragraph) are shown.

Although no deductions concerning the depositional environment are yet possible by examination of these biomarkers in detail (Mackenzie et al., 1982), we can make some deductions regarding the degree of maturation and possible migration of hydrocarbons (Seifert and Moldowan, 1981). Seifert has studied the transformations of the 14α(H),17α(H)(20R)-geosterane (II, Fig. 12), which is formed from the 14α(H),17α(H)(20R)-sterol (I, Fig. 12) found in living organisms (Nes et al., 1977). The geosterane II is isomerized to its epimer 14α(H), 17α(H)(20S)-geosterane III and to 14β(H),17β(H)(20R)-geosterane IV. The three steranes II, III, and IV (Fig. 12) are of most interest here.

Seifert and Moldowan (1981) have shown that the ratios of the geosteranes III/II plotted versus IV/II can give considerable information regarding the degree of maturation as well as migration. Figure 13 (from their paper) shows a line, the first-order kinetic conversion (maturation) found for a number of oils. The displacement along this line is a measure of the maturity. Migrated oils are displaced to the right of the curve. Shown in Figure 13 are oils from Ship Shoal, Prudhoe Bay, and the Overthrust Belt (Seifert and Moldowan, 1981). The dashed lines are a measure of migration. The displacement to the right of the maturation line is due primarily to the difference in migrational aptitudes of IV and II. The slight slope of the dashed lines is due to the slight difference in migrational aptitude between Compounds III and II, both effects essentially caused by geochromatography effects. Sample 40 (tar/asphalt, 535-58-4, 19–20 cm) is also plotted in Figure 13 and may be compared with the positions of the oils studied by Seifert and Moldowan.

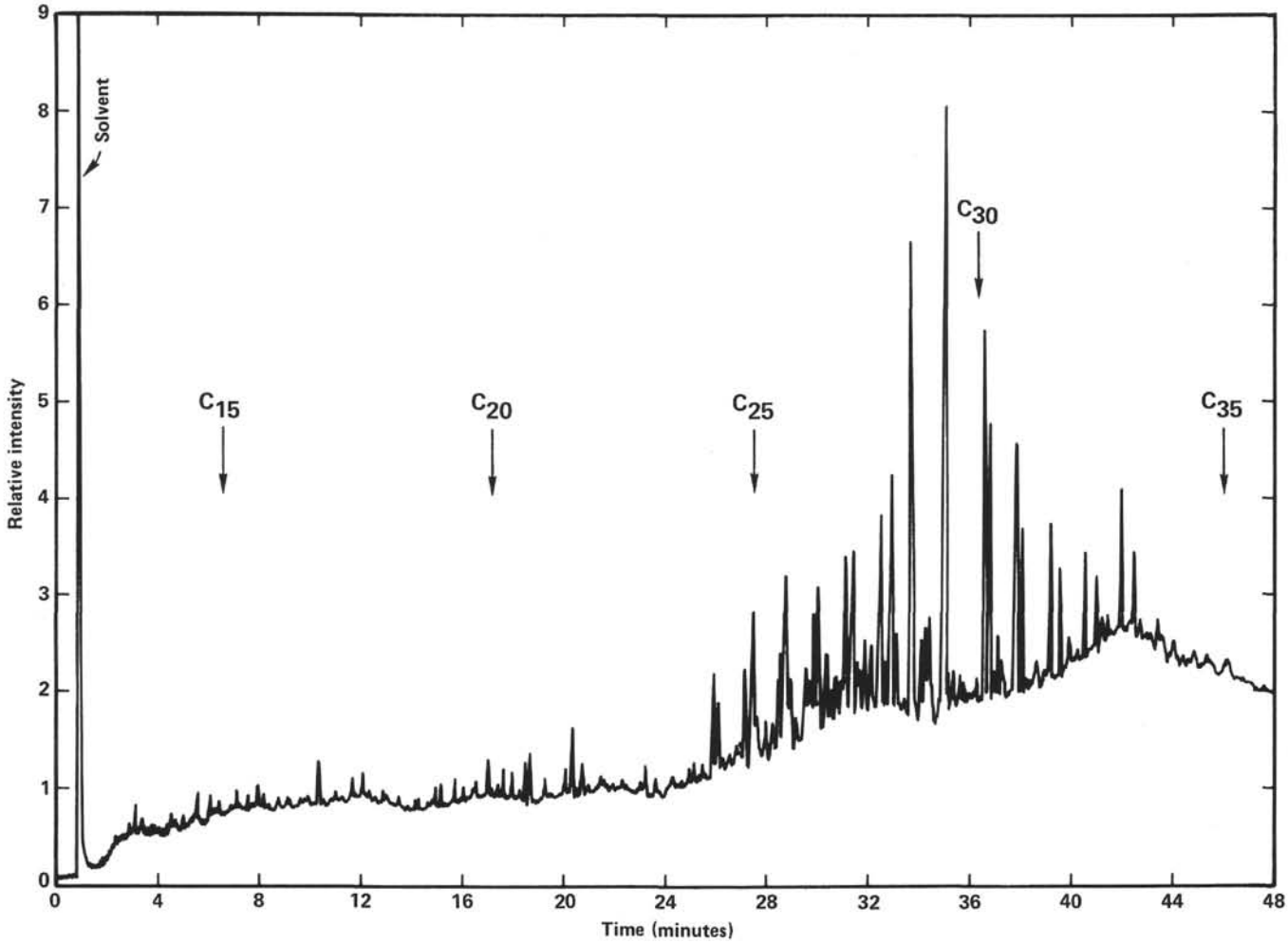


Figure 9. Gas chromatograph of saturate fraction of Sample 40, tar from Sample 535-58-4, 19–20 cm.

It is not clear whether the biodegradation seen in this sample is sufficient to influence the proportions of these geosteranes. The 20S/20R ratio for $C_{27}$ is observed to decrease for heavily degraded oils (Seifert and Moldowan, 1979), but this may not be true for the $C_{29}$ steranes. Indeed, Seifert and Moldowan (1979) state "it is not possible to assign the subtle change in 20S/20R ratio in the regular steranes to different rates of biodegradation because it could mostly or totally be the consequence of different degrees of maturation." If there should be a decrease in the 20S/20R ratio for $C_{29}$ caused by biodegradation of Sample 40, its position in Figure 13 would have been even higher along the biomarker maturation line had it not been biodegraded. At any rate, its degree of maturation is clearly higher than would be expected from the kerogen in adjacent units, clearly supporting its migration from some deeper horizon. The slight shift to the right of the biomarker maturation line may not be very significant. Its small magnitude does suggest relatively little separation of epimers caused by geochromatography effects during migration. But, if this material were expressed through fractures from deeper horizons, such chromatographic effects would be minimal.

At this point, the data appear to support a relatively mature material, with evidence for microbiological alteration, as seen by the lack of *n*-paraffins in the gas chromatographs. The sterane composition supports a mature, migrated classification. Other parameters suggest that the "kerogen" in Sample 16 is heavily stained (contaminated) with this tar/asphalt material.

## GENERAL CONCLUSIONS

This study confirms the findings of the Shipboard Scientific Party that in the sequence of Early Cretaceous to mid-Cretaceous deep-water limestones sampled from cores at Sites 535 and 540, the organic matter is dominantly of Types II and III (Fig. 6). That this organic matter is thermally immature is indicated by both HI:OI ratios (Fig. 6) and visually observed color of the spore-cuticle fraction. Source-rock potential, however, as gaged by the total organic carbon contents (TOC), ranges from fair to very good. Source potential based on TOC and hydrogen content is best in the Early Cretaceous (late Valanginian through Barremian) sequence cored at Site 535.

Throughout, the kerogen fractions of these carbonates are mixtures of marine and terrigenous material. This seems to be true even in the pelagic, foraminifer-rich limestones of the late Albian and early Cenomanian at Site 540 (Samples 28–36), suggesting that the ter-

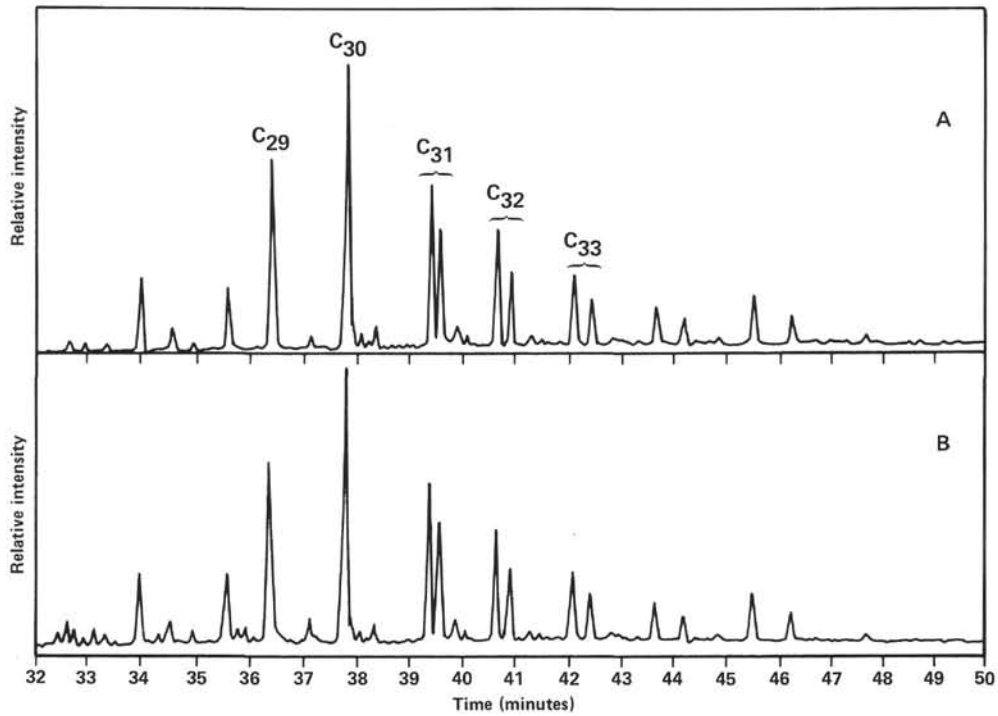


Figure 10. Portion of gas chromatography–mass spectrometry trace of tar/asphalt Sample 40. Fused silica bonded phase DB-1 column. See text for column conditions. A. Mass fragmentogram for m/e = 191, diagnostic for triterpanes. Carbon numbers of principle peaks indicated. B. Total ionization in selective ion monitoring mode, m/e = 57, 191, and 217.

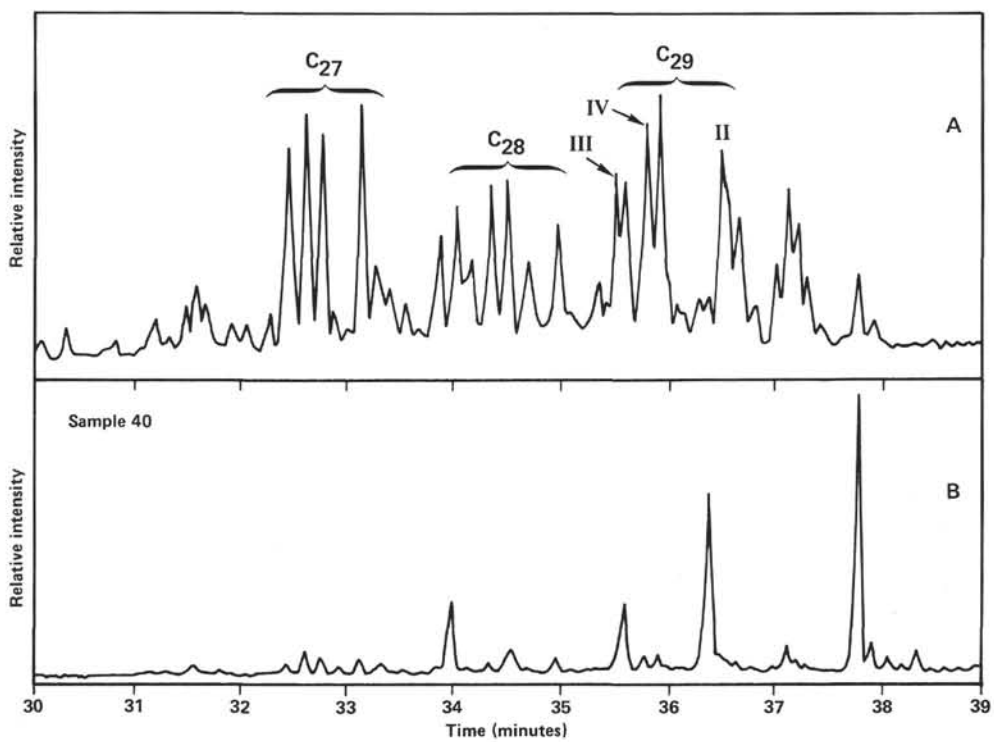


Figure 11. Portion of gas chromatography/mass spectrometry trace of tar/asphalt Sample 40. Fused silica bonded phase DB = 1 column. See text for column conditions. A. Mass fragmentogram for m/e = 217, diagnostic for steranes. Carbon numbers of principle peaks indicated. Compounds II = 14$\alpha$, 17$\alpha$(20R) = geosterane, III = 14$\alpha$,17$\alpha$(20S) = geosterane, IV = 14$\beta$,17$\beta$(20R) = geosterane. See text for further details. B. Total ionization in selective ion monitoring mode, m/e = 57, 191, and 217.

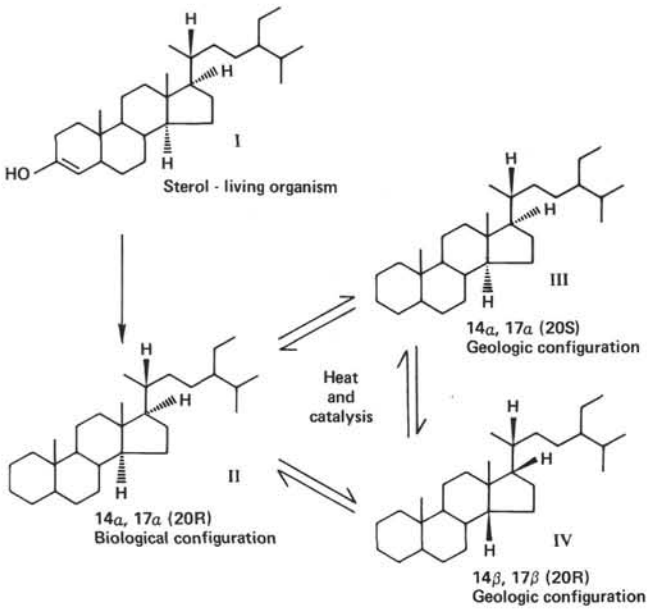


Figure 12. $C_{29}$ steranes useful for maturation/migration evaluation of oils and extracts (after Seifert and Moldowan, 1981).

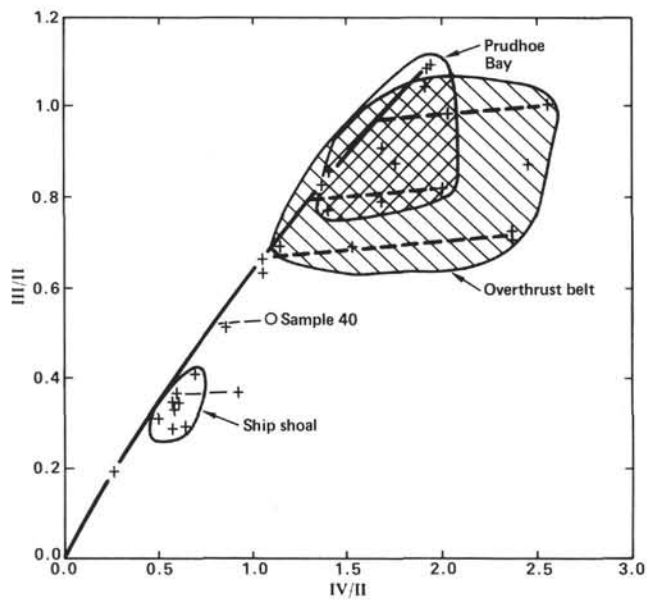


Figure 13. Biomarker maturation index (BMAI) and biomarker migration (BMII) lines and data for several crude oils from Seifert and Moldowan (1981). Ratios of $C_{29}$ steranes III/II plotted versus IV/II. See Figure 12 for identification. Tar/asphalt Sample 40 plotted with these data.

rigenous component is a refractory background. However, variations in the types of amorphous kerogen, and in their relative abundances compared with other kerogens, are reflected in the compositions of pyrolyzed hydrocarbons and the ratios of hydrogen to oxygen in organic fractions.

The sediments in this suite of dominantly dark, organic matter–rich carbonates can be divided into three major groupings: (1) lime mudstones (marls) that are poorly laminated, light to medium colored, and only moderately rich in organic matter and that have small but omnipresent fractions of terrigenous quartz-rich silt (Berriasian and early Valanginian, Samples 18, 19, and 22–26); (2) marls that are very well laminated, medium to very dark colored, and moderately to highly rich in organic matter and that have very sparse or trace amounts of terrigenous silt and an abundance of compacted, micritic pellets probably of fecal origin (Samples 21, 22); and (3) dark, silt-free, pelagic limestones with an abundance of both fecal pellets and planktonic foraminifers (Samples 28–36).

Pyrolysis mass spectrometry in conjunction with other geochemical analyses gives a detailed picture of the nature of the organic matter and the degree to which its depositional and early diagenetic environments were reducing (anoxic) or oxidizing. The resulting geochemical interpretations are consistent with the scenario suggested by the visual kerogen and sedimentologic evaluations. All of our interpretations are consistent with the picture of alternating anoxic and oxic sedimentary events in these basinal sites, and are compatible with the major anoxic Cretaceous events found by other researchers.

Anoxic events, in addition to suitable organic matter, appear to be critical for good source-rock quality in this sequence of fine-grained deep-sea carbonates. Given a particular "reservoir" of organic matter, strongly reducing conditions produce the most oil-prone kerogen.

The tar/asphalt sample from Section 535-58-4 appears to have been biodegraded and is relatively mature. It also appears not to have been formed in place but to have been extruded into the fractures in the rock, probably from lower sections.

## ACKNOWLEDGMENTS

We wish to express our thanks to H. M. Heck for help with the kerogen residue slides, to H. Maxwell, Jr., and L. B. Smith for mass spectral assistance, to D. D. Wallwey for obtaining the isotopic carbon data, to Dr. W. M. Benzel and N. L. Neafus for the X-ray determinations, and to K. A. Lintelmann for liquid chromatography separations.

## REFERENCES

Arthur, M. A., and Schlanger, S. O., 1979. Cretaceous "Oceanic Anoxic Events" as causal factors in development of reef-reservoired giant oil fields. *Am. Assoc. Pet. Geol. Bull.*, 63:870–885.

Bein, A., and Reiss, Z., 1976. Cretaceous *Pithonella* from Israel. *Micropaleontology,* 22:83–91.

Demaison, G. J., and Moore, G. T., 1980. Anoxic environments and oil source bed genesis. *Am. Assoc. Pet. Geol. Bull.*, 64:1179–1209.

Dunham, R. J., 1962. Classification of carbonate rocks according to depositional texture. *In* Ham, W. E. (Ed.), *Classification of Carbonate Rocks—A Symposium:* Tulsa, Oklahoma (Am. Assoc. Pet. Geol. Mem.), 1:108–121.

Mackenzie, A. S., Brassell, S. C., Eglinton, G., and Maxwell, J. R., 1982. Chemical fossils: the geological fate of steroids. *Science,* 217: 491–504.

Marszalek, D. S., 1975. Calcisphere ultrastructure and skeletal aragonite from the algal *Acetabularia antillana. J. Sediment. Petrol.*, 45: 266–271.

Nes, W. R., Varkey, T. E., and Krevitz, K., 1977. The stereochemistry of sterols at C-20 and its biosynthetic implications. J. Am. Chem. Soc., 99:260–261.

Orr, W. L., 1974. Changes in sulfur content and isotopic ratios of sulfur during petroleum maturation—Study of Big Horn Basin Paleozoic oils. Part 1. *Am. Assoc. Pet. Geol. Bull.*, 58:2295–2318.

Patton, J. W., and Moore, A., 1982. Thermolysis/mass spectrometry of kerogen [paper presented at the Fifth Int. Sym. Anal. Pyrolysis, Vail, Colorado].

Robinson, C. J., 1971. Low-resolution mass spectrometric determination of aromatics and saturates in petroleum fractions. *Anal. Chem.*, 43:1425–1434.

Rupp, A. W., 1967. Origin, structure, and environmental significance of Recent and fossil calcispheres. *Geol. Soc. Am. Spec. Pap.*, 101: 186. (Abstract)

Schlager, W., Buffler, R. T., and Shipboard Scientific Party, 1984. DSDP Leg 77, southeastern Gulf of Mexico. *Geol. Soc. Am. Bull.*, 95:226–236.

Seifert, W. K., and Moldowan, J. M., 1979. The effect of biodegradation on steranes and terpanes in crude oils. *Geochim. Cosmochim. Acta,* 43:111–126.

Seifert, W. K., and Moldowan, J. M., 1981. Paleoreconstruction by biological markers. *Geochim. Cosmochim. Acta,* 45:783–794.

Shinn, E. A., Halley, R. B., Hudson, J. M., and Lidz, B. H., 1977. Limestone compaction—an enigma. *Geology,* 5:21–24.

Shinn, E. A., and Robbin, D. M., in press. Compaction, pressure solution, and lithification in fine-grained shallow-water limestones. *J. Sediment. Petrol.*

Souron, C., Boulet, R., and Espitalie, J., 1974. Etude par spectromètrie de masse de la décomposition thermique sous vide de kerogenes appartenant a deux lignees evolutives distinctes. *Rev. Inst. Fr. Pet.*, 24:661–678.

Tissot, B., Demaison, B., Masson, P., Delteil, J. R., and Combaz, A., 1980. Paleoenvironment and petroleum potential of Middle Cretaceous black shales in Atlantic basins. *Am. Assoc. Pet. Geol. Bull.*, 64:2051–2063.

Wray, J. L., 1977. *Calcareous Algae:* New York (Elsevier, Scient. Publ. Co.).

**Date of Initial Receipt: January 17, 1983**
**Date of Acceptance: June 24, 1983**

## APPENDIX A
### Carbon Analyses and Rock-Eval Geochemical Data

| Sample number | Depth (m) | Organic carbon (%) | Carbonate carbon (%) | $S_1$ (mg/g) | $S_2$ (mg/g) | $S_3$ (mg/g) | Temperature (°C) ($S_2$ maximum) |
|---|---|---|---|---|---|---|---|
| 27 | 141.7 | 2.46 | 5.76 | 0.169 | 5.08 | 4.50 | 404 |
| 28 | 337.5 | 0.94 | 9.64 | 0.021 | 3.21 | 1.12 | 417 |
| 29 | 339.0 | 2.37 | 10.72 | 0.094 | 10.39 | 1.72 | 408 |
| 30 | 386.3 | 2.55 | 10.75 | 0.053 | 13.37 | 1.77 | 391 |
| 31 | 394.5 | 2.83 | 10.54 | 0.047 | 15.57 | 1.80 | 407 |
| 32 | 405.7 | 2.13 | 7.36 | 0.140 | 14.98 | 2.00 | 401 |
| 33 | 413.5 | 2.51 | 10.51 | 0.045 | 6.00 | 1.69 | 407 |
| 34 | 415.4 | 3.16 | 10.11 | 0.069 | 7.04 | 2.33 | 403 |
| 35 | 423.3 | 2.57 | 10.13 | 0.073 | 7.97 | 1.26 | 424 |
| 36 | 432.8 | 1.60 | 10.26 | 0.071 | 6.67 | 1.36 | 414 |
| 37 | 442.9 | 0.86 | 10.99 | 0.047 | 3.54 | 0.83 | 420 |
| 38 | 462.5 | 0.58 | 11.08 | 0.030 | 2.51 | 0.84 | 413 |
| 39 | 584.8 | 1.21 | 10.56 | 0.081 | 4.67 | 1.06 | 420 |
| 1 | 287.0 | 0.74 | 7.06 | 0.049 | 0.64 | 2.33 | 409 |
| 2 | 322.1 | 3.81 | 7.21 | 0.012 | 9.63 | 3.00 | 414 |
| 3 | 380.3 | 2.97 | 8.95 | 0.030 | 14.32 | 2.05 | 414 |
| 4 | 388.8 | 2.57 | 5.82 | 0.002 | 7.89 | 2.10 | 415 |
| 5 | 402.0 | 1.31 | 9.60 | 0.061 | 3.21 | 1.37 | 412 |
| 6 | 457.3 | 3.53 | 5.78 | 0.065 | 11.77 | 2.03 | 399 |
| 7 | 458.3 | 4.04 | 4.96 | 0.210 | 19.04 | 2.22 | 413 |
| 8 | 458.3 | 0.59 | 0.39 | 0.169 | 1.63 | 0.63 | 412 |
| 9 | 458.3 | 6.58 | 3.52 | 0.270 | 21.80 | 3.60 | 417 |
| 10 | 473.7 | 1.68 | 6.90 | 0.031 | 4.59 | 2.13 | 417 |
| 11 | 480.7 | 1.49 | 9.21 | 0.019 | 4.90 | 1.17 | 411 |
| 12 | 495.1 | 2.60 | 8.03 | 0.000 | 4.56 | 1.90 | 411 |
| 13 | 501.6 | 2.34 | 7.82 | 0.000 | 16.03 | 1.61 | 403 |
| 14 | 512.8 | 2.81 | 6.64 | 0.024 | 12.63 | 2.54 | 406 |
| 15 | 527.6 | 3.14 | 6.69 | 0.000 | 24.10 | 3.17 | 393 |
| 16 | 529.8 | 1.45 | 10.36 | 0.737 | 7.42 | 0.85 | 417 |
| 17 | 552.3 | 4.70 | 8.05 | 0.013 | 26.27 | 2.59 | 395 |
| 18 | 575.5 | 4.05 | 6.88 | 0.051 | 19.00 | 2.28 | 401 |
| 19 | 584.2 | 5.52 | 5.79 | 0.000 | 19.41 | 2.55 | 402 |
| 20 | 598.8 | 2.44 | 7.80 | 0.050 | 10.26 | 2.38 | 417 |
| 21 | 608.8 | 1.30 | 8.66 | 0.032 | 8.22 | 1.67 | 413 |
| 22 | 617.6 | 1.54 | 7.54 | 0.047 | 5.62 | 1.80 | 410 |
| 23 | 626.1 | 1.20 | 5.59 | 0.016 | 4.45 | 1.13 | 414 |
| 24 | 632.9 | 1.12 | 7.78 | 0.041 | 3.13 | 1.60 | 421 |
| 25 | 641.6 | 2.18 | 7.43 | 0.074 | 5.39 | 1.71 | 408 |
| 26 | 696.9 | 1.28 | 5.79 | 0.051 | 4.24 | 1.49 | 424 |
| 40 | 529.1 | 73.2 | | | | | |

Note: Carbon analyses by Huffman Laboratories; Rock-Eval data from G. E. Claypool, U.S.G.S. See Table 1 for DSDP sample designations.

## APPENDIX B
### Rock-Eval and Isotopic Carbon Geochemical Data

| Sample number | Hydrogen index | Oxygen index | Production index $[S_1/(S_1 + S_2)]$ | Oil/gas index ($S_2/S_3$) | $\delta^{13}C$ Organic carbon (‰) | $\delta^{13}C$ Carbonate carbon (‰) |
|---|---|---|---|---|---|---|
| 27 | 207 | 183 | 0.032 | 1.13 | −24.22 | 2.54 |
| 28 | 341 | 119 | 0.006 | 2.87 | −25.42 | 3.42 |
| 29 | 438 | 73 | 0.009 | 6.04 | −25.93 | 2.92 |
| 30 | 524 | 69 | 0.004 | 7.55 | −26.07 | 2.06 |
| 31 | 550 | 64 | 0.003 | 8.65 | −25.86 | 1.72 |
| 32 | 703 | 98 | 0.009 | 7.17 | −26.96 | 2.21 |
| 33 | 239 | 67 | 0.007 | 3.55 | −26.45 | 1.75 |
| 34 | 223 | 74 | 0.010 | 3.02 | −26.51 | 1.99 |
| 35 | 310 | 49 | 0.009 | 6.33 | −24.50 | 2.00 |
| 36 | 417 | 85 | 0.011 | 4.90 | −24.66 | 2.00 |
| 37 | 412 | 97 | 0.013 | 4.27 | −23.92 | 2.67 |
| 38 | 433 | 145 | 0.012 | 2.99 | −23.89 | 2.90 |
| 39 | 386 | 88 | 0.017 | 4.41 | −24.97 | 2.46 |
| 1 | 86 | 315 | 0.071 | 0.27 | −24.96 | 3.29 |
| 2 | 253 | 79 | 0.001 | 3.21 | −26.65 | 2.62 |
| 3 | 482 | 69 | 0.002 | 6.99 | −25.79 | 2.65 |
| 4 | 307 | 82 | 0.000 | 3.76 | −25.99 | 1.70 |
| 5 | 245 | 105 | 0.019 | 2.34 | −27.03 | 2.07 |
| 6 | 333 | 58 | 0.005 | 5.80 | −26.75 | 1.36 |
| 7 | 471 | 55 | 0.011 | 8.58 | −28.08 | 1.62 |
| 8 | 276 | 107 | 0.094 | 2.59 | −27.95 | 2.13 |
| 9 | 331 | 55 | 0.012 | 6.06 | −28.21 | 1.72 |
| 10 | 273 | 127 | 0.007 | 2.15 | −27.38 | 1.52 |
| 11 | 329 | 79 | 0.004 | 4.19 | −26.91 | 2.06 |
| 12 | 175 | 73 | 0.000 | 2.40 | −27.90 | 1.25 |
| 13 | 685 | 69 | 0.000 | 9.96 | −27.89 | 1.75 |
| 14 | 449 | 90 | 0.002 | 4.97 | −27.39 | 1.78 |
| 15 | 768 | 101 | 0.000 | 7.60 | −27.58 | 1.68 |
| 16 | 512 | 59 | 0.090 | 8.73 | −25.92 | 1.69 |
| 17 | 559 | 55 | 0.000 | 10.14 | −26.60 | 2.36 |
| 18 | 469 | 56 | 0l003 | 8.33 | −27.12 | 2.71 |
| 19 | 352 | 46 | 0.000 | 7.61 | −26.89 | 2.46 |
| 20 | 420 | 98 | 0.005 | 4.31 | −27.36 | 2.26 |
| 21 | 632 | 128 | 0.004 | 4.92 | −26.68 | 2.34 |
| 22 | 365 | 117 | 0.008 | 3.12 | −28.32 | 1.66 |
| 23 | 371 | 94 | 0.004 | 3.94 | −28.35 | 1.62 |
| 24 | 279 | 143 | 0.013 | 1.96 | −28.55 | 1.00 |
| 25 | 247 | 78 | 0.014 | 3.15 | −28.65 | 1.10 |
| 26 | 331 | 116 | 0.012 | 2.85 | −28.24 | 1.77 |
| 40 | | | | | −25.63 | |

Note: Rock-Eval data from G. E. Claypool, U.S.G.S.; carbon isotope data from D. Wallwey, Marathon Oil. $\delta^{13}C$ values versus PDB standard. See Table 1 for equivalent DSDP sample numbers.

## APPENDIX C
### Pyrolysis Mass Spectral Data

| Sample number | Paraffins (%) | Naphthenes (%) | Aromatics (%) | Napthenes | | | $PS_1$ | $PS_2$ | PHI | PPI (%) | RI |
|---|---|---|---|---|---|---|---|---|---|---|---|
| | | | | Monocyclics (%) | Dicyclics (%) | Tricyclics + (%) | | | | | |
| 27 | 12.2 | 66.6 | 21.2 | 29.7 | 8.3 | 62.0 | 0.78 | 11.7 | 4.8 | 6.2 | 1.54 |
| 28 | 5.9 | 66.1 | 27.9 | 26.8 | 7.3 | 65.9 | 0.05 | 10.0 | 10.6 | 3.9 | 2.29 |
| 29 | 6.0 | 63.8 | 30.0 | 24.1 | 4.5 | 71.3 | 2.75 | 25.9 | 10.9 | 9.6 | 5.17 |
| 30 | 4.7 | 59.7 | 35.5 | 24.5 | 13.0 | 61.9 | 1.55 | 31.6 | 12.4 | 4.7 | 6.86 |
| 31 | 5.6 | 61.6 | 32.7 | 25.8 | 14.4 | 59.7 | 2.03 | 29.4 | 10.4 | 6.5 | 4.84 |
| 32 | 5.4 | 61.8 | 32.8 | 22.8 | 11.3 | 65.9 | 2.50 | 19.8 | 9.3 | 11.2 | 5.52 |
| 33 | 3.1 | 59.5 | 37.3 | 24.9 | 13.6 | 61.5 | 0.68 | 18.5 | 7.4 | 3.6 | 4.45 |
| 34 | 4.8 | 59.5 | 35.7 | 32.3 | 16.3 | 52.4 | 8.10 | 28.6 | 9.0 | 22.1 | 4.89 |
| 35 | 6.8 | 63.9 | 29.3 | 27.9 | 15.5 | 56.6 | 2.42 | 18.7 | 7.3 | 11.5 | 3.03 |
| 36 | 8.9 | 63.2 | 27.7 | 30.7 | 14.9 | 54.4 | 0.14 | 10.5 | 6.6 | 1.3 | 1.96 |
| 37 | 8.3 | 62.7 | 28.9 | 32.2 | 16.3 | 57.5 | 0.82 | 10.8 | 12.5 | 7.1 | 1.03 |
| 38 | 10.8 | 66.1 | 23.1 | 34.3 | 8.9 | 56.7 | 0.85 | 6.7 | 11.6 | 11.2 | 0.84 |
| 39 | 9.4 | 63.8 | 26.8 | 32.6 | 16.1 | 51.3 | 0.79 | 9.2 | 7.6 | 7.9 | 1.27 |
| 1 | 6.2 | 72.8 | 21.1 | 41.6 | 11.4 | 47.0 | 0.05 | 3.7 | 5.0 | 1.4 | 0.78 |
| 2 | 2.3 | 56.7 | 41.9 | 23.8 | 6.2 | 70.0 | 0.53 | 20.3 | 5.3 | 2.5 | 6.13 |
| 3 | 2.5 | 60.3 | 31.9 | 29.0 | 7.3 | 63.7 | 1.63 | 20.1 | 6.8 | 7.5 | 4.14 |
| 4 | 10.6 | 59.8 | 29.7 | 36.6 | 8.5 | 54.8 | 3.35 | 21.1 | 8.2 | 13.7 | 3.86 |
| 5 | 8.9 | 63.2 | 27.9 | 34.5 | 7.6 | 57.9 | 0.89 | 10.1 | 7.7 | 8.1 | 1.15 |
| 6 | 7.7 | 60.8 | 31.5 | 29.9 | 9.5 | 60.5 | 0.67 | 18.9 | 5.3 | 3.4 | 5.58 |
| 7 | 6.0 | 57.8 | 36.3 | 28.2 | 7.1 | 64.7 | 2.60 | 25.6 | 6.3 | 9.2 | 6.00 |
| 8 | 7.2 | 58.9 | 33.9 | 30.6 | 15.8 | 53.6 | 0.64 | 4.6 | 7.8 | 12.2 | 1.09 |
| 9 | 5.9 | 59.2 | 34.8 | 33.1 | 7.3 | 59.6 | 5.05 | 56.7 | 8.6 | 8.2 | 15.5 |
| 10 | 8.1 | 65.2 | 26.7 | 29.1 | 5.8 | 65.0 | 1.85 | 9.0 | 5.3 | 17.1 | 2.40 |
| 11 | 6.2 | 63.2 | 30.7 | 25.9 | 7.3 | 66.8 | 0.69 | 9.0 | 6.1 | 7.1 | 2.98 |
| 12 | 3.5 | 54.8 | 41.6 | 23.7 | 5.3 | 71.0 | 1.00 | 19.0 | 7.3 | 5.0 | 3.77 |
| 13 | 5.4 | 60.0 | 34.5 | 26.5 | 14.8 | 58.7 | 0.36 | 15.4 | 6.6 | 2.3 | 4.27 |
| 14 | 6.3 | 61.2 | 32.6 | 26.0 | 5.1 | 68.9 | 1.41 | 18.1 | 6.4 | 7.2 | 4.73 |
| 15 | 5.8 | 58.7 | 35.4 | 29.1 | 6.3 | 64.1 | 0.65 | 19.5 | 6.2 | 3.2 | 4.34 |
| 16 | 11.8 | 50.1 | 38.1 | 34.1 | 32.1 | 33.7 | 3.32 | 11.5 | 7.9 | 22.4 | 1.10 |
| 17 | 5.3 | 57.1 | 37.6 | 25.4 | 7.4 | 67.2 | 5.29 | 36.0 | 7.7 | 12.8 | 8.67 |
| 18 | 5.7 | 58.3 | 36.0 | 28.6 | 10.1 | 61.2 | 1.42 | 26.9 | 6.6 | 5.0 | 6.48 |
| 19 | 6.5 | 57.6 | 35.9 | 28.5 | 5.2 | 66.3 | 1.34 | 47.7 | 8.6 | 2.7 | 12.3 |
| 20 | 5.1 | 63.5 | 31.4 | 26.9 | 5.7 | 67.4 | 0.80 | 15.7 | 6.4 | 4.8 | 5.17 |
| 21 | 10.1 | 68.6 | 21.3 | 32.4 | 7.0 | 60.6 | 0.47 | 7.7 | 5.9 | 5.7 | 1.96 |
| 22 | 10.9 | 67.3 | 21.7 | 32.7 | 3.9 | 63.4 | 0.85 | 9.3 | 6.0 | 8.4 | 2.58 |
| 23 | 11.8 | 66.6 | 21.6 | 35.4 | 3.3 | 61.3 | 0.64 | 6.8 | 5.6 | 8.7 | 1.98 |
| 24 | 12.5 | 67.7 | 19.9 | 33.8 | 6.1 | 60.1 | 0.96 | 7.0 | 6.3 | 12.0 | 1.79 |
| 25 | 9.4 | 59.9 | 30.7 | 30.1 | 5.3 | 64.6 | 0.55 | 17.4 | 8.0 | 3.1 | 4.40 |
| 26 | 11.4 | 64.9 | 23.8 | 36.2 | 10.9 | 52.9 | 0.51 | 8.9 | 7.0 | 5.4 | 2.34 |
| 40 | 13.7 | 47.1 | 39.2 | 33.3 | 28.8 | 38.6 | 339. | 627. | 8.6 | 35.1 | 18.5 |

Note: Analysts were A. J. Kaltenback, H. Maxwell, Jr., A. Moore, and J. W. Patton. Data based on mass spectral data from pyrolyses between 300° and 600°C paraffin = napthene-aromatic (PNA) data and napthene data calculated by method of Robinson (1971). "Tricyclics +" means tricyclics and higher cyclics. $PS_1$ = pyrolysis $S_1$ index; $PS_2$ = pyrolysis $S_2$ index; PHI = pyrolysis hydrocarbon index; PPI = pyrolysis production index; RI = reduction index. All of these values are in arbitrary units/$\mu$g of rock, unless otherwise indicated. See text for details.

**APPENDIX D**
**Semiquantitative Compositions of Kerogen Constitutents and Inorganic Constituents in Study Samples**

| | | | | | Residue slide mount | | | | | | | | | | Thin section | | | | | | |
|---|---|---|---|---|---|---|---|---|---|---|---|---|---|---|---|---|---|---|---|---|---|
| | | | | | Gas prone | | | Oil prone | | | | | | | | | | | | | |
| Sample number | Hole | Core-section | Age | Total organic carbon (%) | Fusinite | Vitrinite | Pyrobitumen | Amorphous | Spores | Cuticle | Dinoflagellates | Microforams | Fungi | Planktonic foraminifers | Compacted pellets | Dolomite | Calcispheres | Radiolarians | Silica (replacement or pore fill) | Terrigenous silt |
| 27 | 538A | 16-5 | late Eocene | 2.46 | S | S | S | A | T | | T | T | T | C | | | | A | C | |
| 28 | 540 | 37-1 | early Cenomanian | 0.94 | S | S | S | S | T | | | T | | C | S | S | | C | S | C |
| 29 | | 37-2 | early Cenomanian | 2.37 | C | S | S | A | T | | | | | A | D | S | | | | S |
| 30 | | 42-2 | late Albian | 2.55 | C | S | S | A | T | | | T | | A | A | | | | | S |
| 31 | | 43-1 | | 2.83 | C | S | S | A | T | | | T | T | D | D | | | | | |
| 32 | | 44-2 | | 2.13 | C | S | S | A | T | T | | T | T | A | A | | | | | |
| 33 | | 45-1 | | 2.15 | C | S | S | A | | | | S | T | C | D | | | | | |
| 34 | | 45-2 | | 3.16 | C | S | S | A | T | T | | | | C | D | | | | | |
| 35 | | 46-1 | | 2.57 | C | S | S | A | T | | T | S | | C | A | S | | | | |
| 36 | | 47-1 | | 1.60 | S | S | S | C | | | | T | | A | D | S | | | | |
| 37 | | 48-1 | | 0.86 | S | S | S | C | T | T | | S | T | S | C | | | | | |
| 38 | | 50-2 | | 0.58 | S | S | S | S | | | S | C | T | S | S | S | | | | |
| 39 | | 63-1 | | 1.21 | S | S | C | C | | | | C | | S | C | | | | | S |
| 1 | 535 | 31-7 | Cenomanian(?) | 0.74 | T | T | T | T | | | | S | T | S | | | | | | |
| 2 | | 35-5 | | 3.81 | S | S | S | A | | | | | | S | A | | | | | |
| 3 | | 41-5 | | 2.97 | S | S | S | A | T | | T | T | S | C | | | | | | S |
| 4 | | 42-5 | | 2.57 | S | S | S | A | | | S | S | T | S | C | S | S | | | |
| 5 | | 44-1 | Aptian | 1.31 | S | S | S | C | | | T | | | S | D | S | | | | |
| 6 | | 50-2 | | 3.53 | S | S | S | A | | | | | T | | A | S | | | | S |
| 7 | | 50-3A | | 4.04 | C | C | C | D | T | T | | | | S | C | | | | | |
| 8 | | 50-3B | | 0.59 | S | S | S | A | T | | | | | S | S | | S | | D | |
| 9 | | 50-3C | | 6.58 | C | C | C | D | T | T | | | | | C | S | S | | | |
| 10 | | 52-1 | Barremian to late Hauterivian | 1.68 | S | S | S | C | S | T | | S | | S | C | S | | | | S |
| 11 | | 53-3 | | 1.49 | S | S | S | C | | | | | | | C | C | S | | | |
| 12 | | 54-6 | | 2.60 | S | S | S | A | | | | | | | D | | S | | | S |
| 13 | | 55-4 | | 2.34 | S | S | S | A | T | | | | | | D | C | | | | S |
| 14 | | 56-5 | | 2.81 | S | S | S | A | T | | | | | | C | S | | | | S |
| 15 | | 58-2 | | 3.14 | C | S | C | C | | | | | T | | D | | S | | | |
| 16 | | 58-4 | | 1.45 | S | S | S | C | | | | | | | | S | A | | | |
| 17 | | 61-1 | late Valanginian | 4.70 | C | C | C | D | | | | | | | D | S | S | | | |
| 18 | | 63-4 | | 4.05 | C | C | C | D | T | | | | | | A | S | | | | S |
| 19 | | 64-4 | | 5.52 | C | C | C | D | T | | | | | | A | S | | | | S |
| 20 | | 66-2 | | 2.44 | S | S | S | A | T | | | | | | D | | S | | | S |
| 21 | | 67-2 | early Valanginian | 1.30 | S | S | S | C | T | | | T | T | S | C | S | | | | S |
| 22 | | 68-5 | | 1.54 | S | S | S | C | T | | | | | | S | S | S | | | S |
| 23 | | 69-5 | | 1.20 | S | S | S | C | T | T | | T | | | | C | | | | S |
| 24 | | 70-3 | | 1.12 | S | S | S | C | T | | | T | | | S | S | | | | S |
| 25 | | 71-3 | | 2.18 | S | S | S | A | T | | | T | | | | | | | | |
| 26 | | 78-1 | late Berriasian | 1.28 | S | S | S | C | C | | | S | T | | | C | S | | | S |

Note: Kerogen analyses by G. K. Guennel and H. M. Heck; other analyses by P. W. Choquette. Total organic carbon percentages shown for comparison. Abundance symbols: D = dominant (>20%); A = abundant ( 11–20%); C = common (6–10%); S = sparse (1–5%); T = traće (<1%). Percentages apply to inorganic constituents; only approximate percentages assigned to kerogen constituents. Color values of core samples are shown in Figures 4 and 5.

## APPENDIX E
**Semiquantitative Mineralogy of Samples by X-Ray Diffraction Analysis**

| Sample number | Hole | Calcite | Dolomite | Ankerite | Mg-Kutnahorite | Quartz | Gypsum | Pyrite | Illite | Kaolinite |
|---|---|---|---|---|---|---|---|---|---|---|
| 27 | 538A | Ma | | | | T | T | Pt | | |
| 28 | 540 | Mi | | Mi | | Mi | T | | T | |
| 29 | | Ma | | T | | T | | Mi | Pt | |
| 30 | | Ma | | Pt | | Pt | | | | |
| 31 | | Ma | | | | | | | | |
| 32 | | Ma | | | | T | | | | |
| 33 | | Ma | | | | T | | | | |
| 34 | | Ma | | Pt | | | | | | |
| 35 | | Ma | | T | | | | | | |
| 36 | | Ma | | Mi | | T | | | T | |
| 37 | | Ma | | | | Pt | | | | |
| 38 | | Ma | | | | T | | | | |
| 39 | | Ma | | | | Pt | | | | |
| 1 | 535 | Ma | | | | T | | | T | Pt |
| 2 | | Ma | | | | T | T | Mi | T | |
| 3 | | Ma | | Mi | | T | | | T | |
| 4 | | Ma | | T | | T | T | | T | |
| 5 | | Ma | | | | T | Pt | | | |
| 6 | | Ma | | | T | T | Mi | Mi | T | |
| 7 | | Ma | | | Ma | T | Mi | T | Mi | |
| 8 | | T | | | Pt | Ma | | | | |
| 9 | | Ma | T | | Pt | T | Mi | T | Mi | |
| 10 | | Ma | | | Mi | T | Mi | | Mi | |
| 11 | | Ma | Mi | | | T | T | | | |
| 12 | | Ma | T | | | T | | | | |
| 13 | | Ma | Mi | | | T | T | | T | |
| 14 | | Ma | | Pt | | T | T | T | T | |
| 15 | | Ma | | Pt | | T | T | Pt | T | |
| 16 | | Ma | | Mi | | T | Pt | | Pt | |
| 17 | | Ma | | | Pt | T | T | T | T | T |
| 18 | | Ma | T | T | | T | T | T | T | T |
| 19 | | Ma | | T | | Mi | T | T | Mi | Mi |
| 20 | | Ma | | T | | T | Pt | Pt | T | T |
| 21 | | Ma | | T | | T | | Pt | T | T |
| 22 | | Ma | | T | | T | | | T | T |
| 23 | | Mi | | Mi | | T | | | T | T |
| 24 | | T | | T | | T | | | T | T |
| 25 | | Ma | | Pt | | T | | T | T | T |
| 26 | | Mi | | Ma | | T | T | T | T | T |

Note: Ma = major component (>35%); Mi = minor component (15–35%); T = trace (5–15%); Pt = probable trace (<5%); blank = not observed. Bulk samples were analyzed, crushed, and ground to 44-μm particle size. Analyses by W. M. Benzel and N. L. Neafus, Marathon Oil Company, Denver Research Center. See Table 1 for DSDP sample numbers.

## NOTE TO THE PLATES

The following list provides a key to the sample numbers used in the plate captions.

| Sample number | DSDP sample number | Sample number | DSDP sample number |
|---|---|---|---|
| 1 | 535-31-7, 0–14 | 21 | 535-67-2, 126–134 |
| 2 | 535-35-5, 6–20 | 22 | 535-68-5, 109–125 |
| 3 | 535-42-5, 120–130 | 23 | 535-69-5, 60 – 68 |
| 4 | 535-42-5, 23–32 | 24 | 535-70-3, 133–148 |
| 5 | 535-44-1, 80–128 | 25 | 535-71-3, 97–123 |
| 6 | 535-50-2, 77–96 | 26 | 535-78-1, 89–97 |
| 7 | 535-50-3, 27–34a | 27 | 538A-16-5, 21–27 |
| 8 | 535-50-3, 27–34b | 28 | 540-37-1, 44–53 |
| 9 | 535-50-3, 27–34c | 29 | 540-37-2, 46–55 |
| 10 | 535-52-1, 69–85 | 30 | 540-42-2, 27–34 |
| 11 | 535-53-3, 0–32 | 31 | 540-43-2, 60–60 |
| 12 | 535-43-6, 53–72 | 32 | 540-44-2, 74–77 |
| 13 | 535-55-4, 51–72 | 33 | 540-45-1, 50–58 |
| 14 | 535-56-7, 73–87 | 34 | 540-45-2, 93–100 |
| 15 | 535-58-2, 103–108 | 35 | 540-46-1, 74–80 |
| 16 | 535-58-4, 3–46 | 36 | 540-47-1, 78–84 |
| 17 | 535-61-1, 29–42 | 37 | 540-48-1, 138–142 |
| 18 | 535-63-4, 97–115 | 38 | 540-50-2, 38–52 |
| 19 | 535-64-4, 60–86 | 39 | 540-63-1, 80–86 |
| 20 | 535-66-2, 20–39 | 40 | 535-58-4, 19–20 |

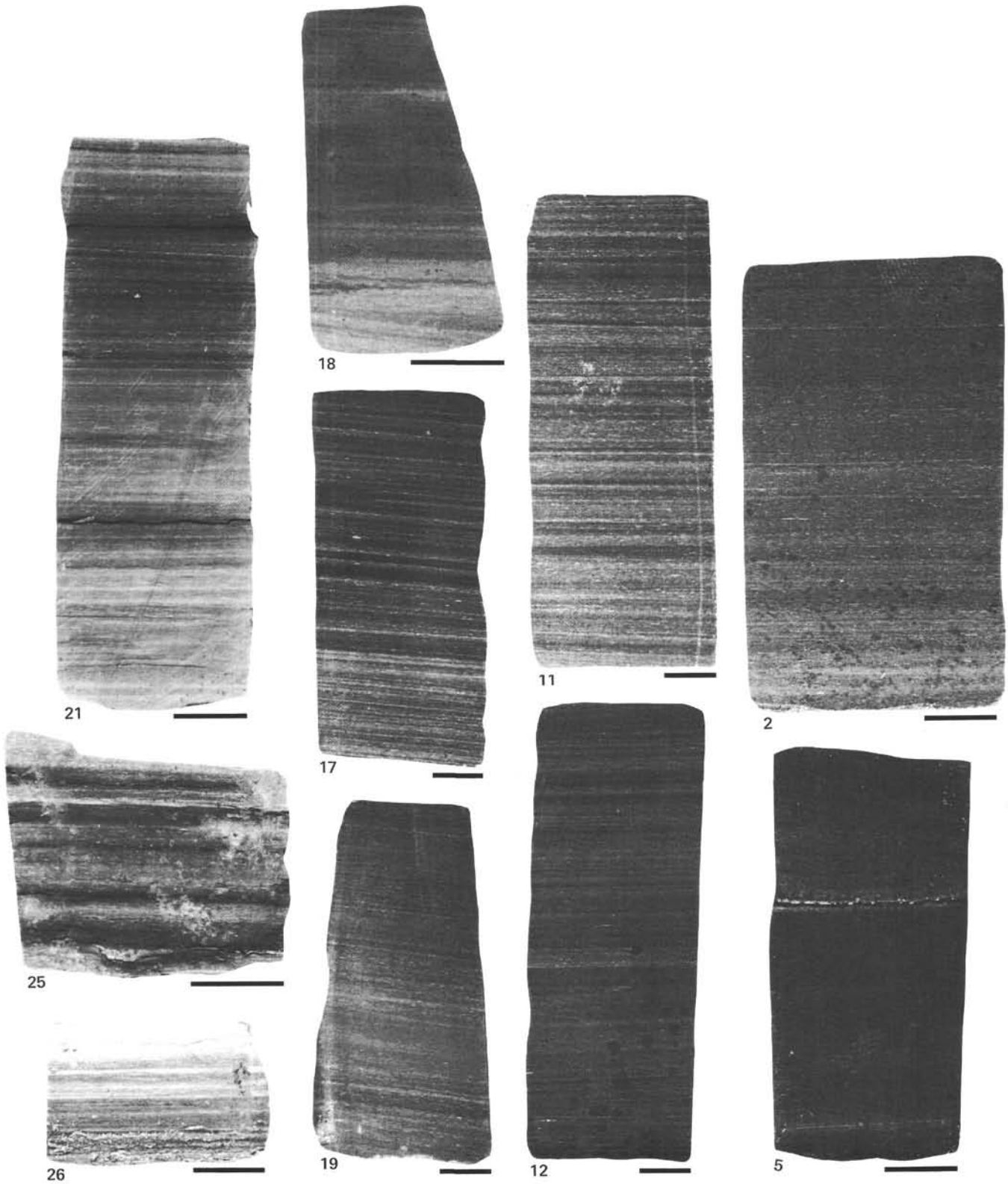


Plate 1. Photographs of sawed surfaces of samples from Lower Cretaceous Units III (Sample 5); IV (Samples 11–12, 17–19, 21); and V (Samples 25–26); and Cenomanian(?) Unit II (Sample 2) from Hole 535. Scale bars indicate 1 cm. In Unit V, light-colored layers show mild bioturbation and predominate slightly over dark, locally bioturbated laminae; cycles appear to be Type E of Buffler and others (this volume) and have lower values for total organic carbon, as expected in a generally oxic environment. Unit IV lithologies tend to be more evenly laminated, show little sign of bioturbation, and exhibit dark-over-light predominance, with cyclically repeated layers of Type A and Type B; seafloor conditions in such cases are interpreted to have been dominantly anoxic (site chapter, Sites 535, 539, and 540, this volume). Samples 2 and 5 contain an abundance of highly compacted, formerly soft pellets (Plate 3, Figs. 3–4) and have more poorly developed sedimentary lamination.

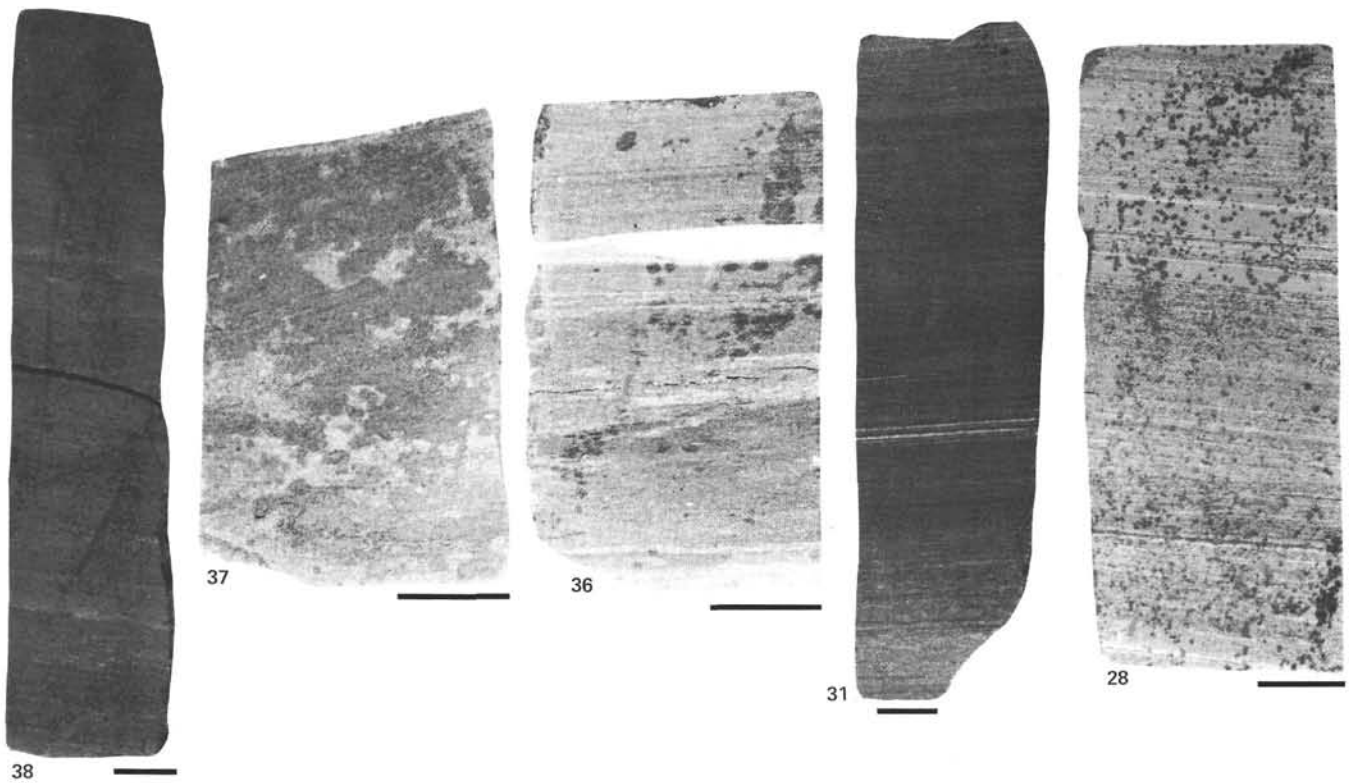


Plate 2. Photographs of sawed surfaces of cores from early Cenomanian (Sample 28) to late Albian (Samples 31–38) Unit IV from Hole 540. Scale bars indicate 1 cm. All but Sample 38 contain assemblages of globigerinids that are empty of materials and, despite compaction of associated pellets, show no signs of crushing (see Plate 5). Samples 36–38 exhibit decreasing bioturbation upward (left to right). Layers of uniform medium-gray micrite in upper part of Sample 28 may represent mud "tails" of distal turbidites.

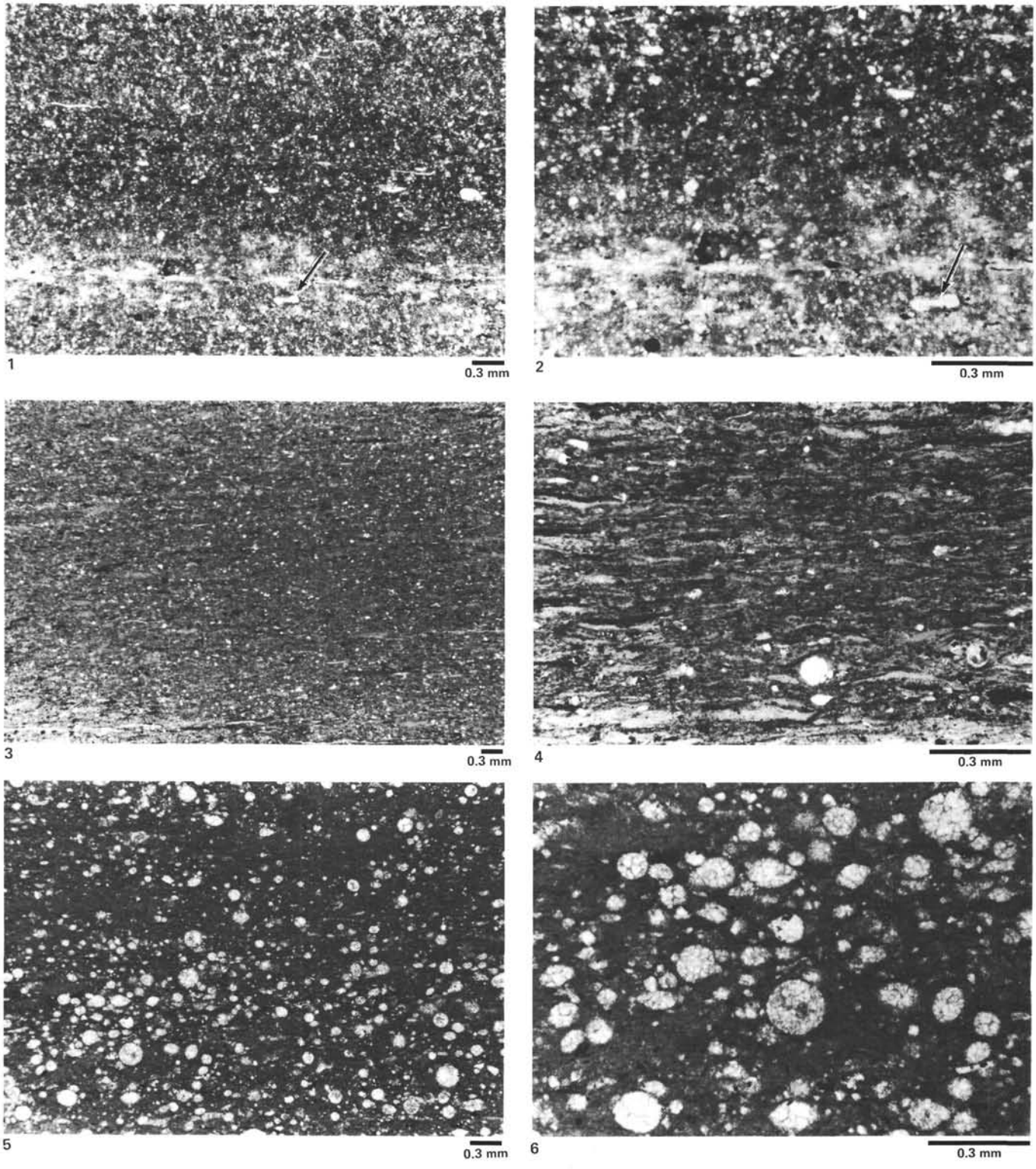


Plate 3. Photomicrographs of carbonate mudstones from Units IV and V, Hole 535; plane light. **1–2.** Lime mudstone with 30% microdolomite rhombs, from a light-colored layer in Sample 26 (Unit V, in Fig. 4); black specks are pyrite; prominent features in both photos shown by arrows. **3–4.** Lime mudstone with very abundant (40% +), highly elongate micritic entities interpreted as compacted fecal(?) pellets; in Figure 4, white object is chalcedonic quartz-filled diatom(?) mold; note also globigerinid foraminifer at far right; this limestone (Sample 15, Unit IV) contains about 3% total organic carbon and 1% pyrite. **5–6.** Calcisphere-rich lime mudstone-wackestone; all calcispheres filled with clear calcite microspar cement; note textural difference in calcisphere to left of center, suggesting either an outer wall and inner cavity or two different concentric tissue layers; Sample 16.

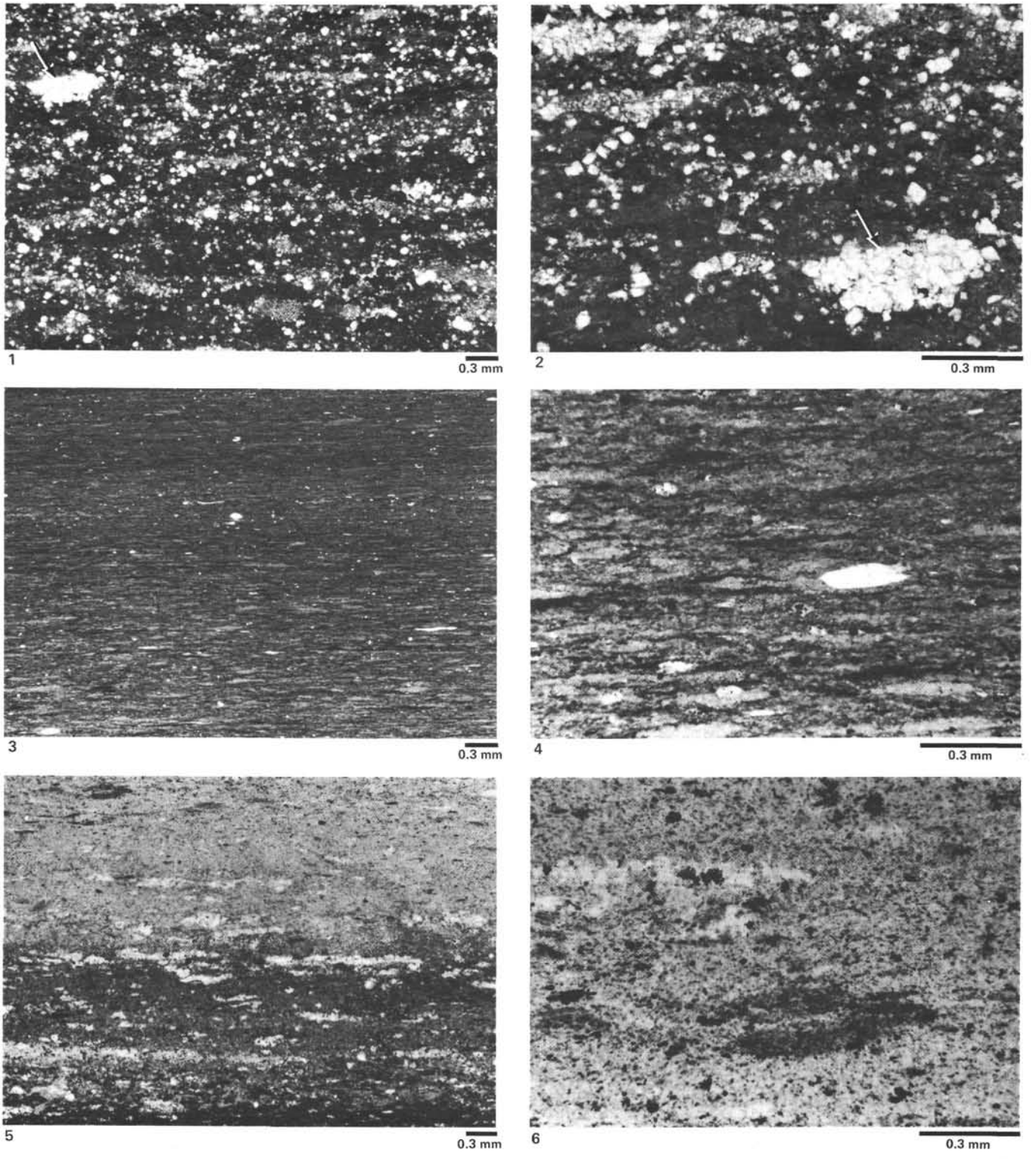


Plate 4. Photomicrographs of carbonates and chert from Units II through IV, Site 535; plane light. **1–2.** Dolomitic limestone with 35% dolomite; discrete "pods" of microdolomite appear to have been burrow fillings; prominent feature in both photos shown by arrows; Sample 11. **3–4.** Compacted-pellet limestone, Sample 5; this lithology is relatively low in organic matter (1.5% total organic carbon); it is interpreted as having been essentially a pellet packstone before compaction but is now a merged-pellet "mudstone;" if pellets were fecal, significant loss of organic matter accompanied compaction; prominent figures in both photos shown by arrows. **5–6.** Chert from nodule, Sample 8; consists of sulfides and assorted organic matter (black), grains and possible micro-burrows (off-white), and matrix (grays), all now altered to chalcedonic quartz.

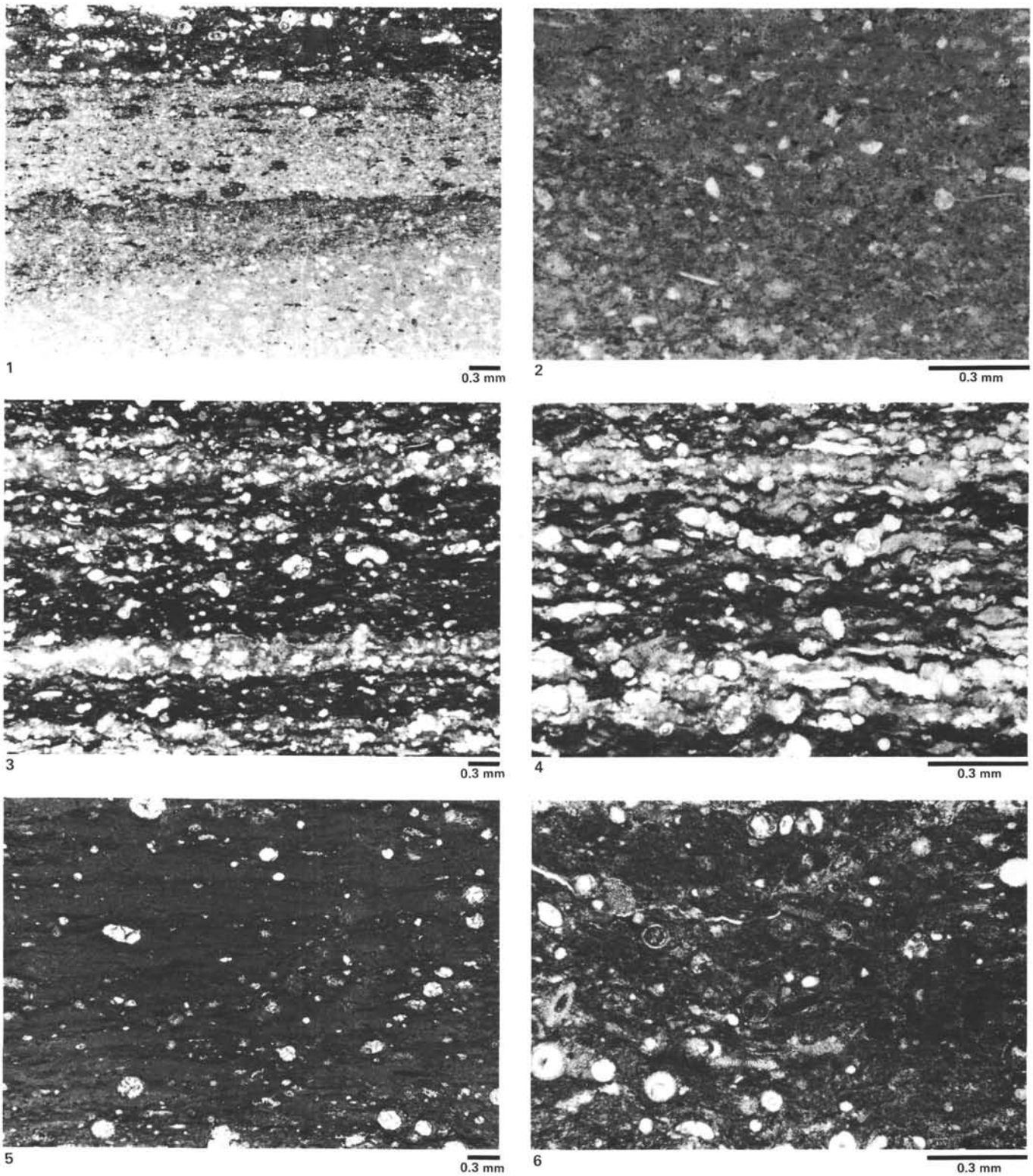


Plate 5. Photomicrographs of lime mudstones from Unit IV, Hole 540, and Unit II, Hole 538A; plane light. **1–2.** Interlayered globigerinid limestone (top) and bioturbated lime mudstone-wackestone; vague grains in photo at right seem to be pellets; Sample 36. **3–4.** Compacted globigerinid limestone (mudstone-wackestone) with dark organic matter; the foraminifers are empty of void-filling cements; Sample 31. **5.** Lime mudstone with scattered chalcedony-filled molds(?) probably of diatoms; Sample 28; moderately compacted and possibly bioturbated. **6.** Lime mudstone-wackestone with abundant diatoms and scattered radiolarians; preserved tests are opal, and a few (white interiors) are hollow; moderately compacted; Sample 27.